



(51) International Patent Classification:

A61K 39/215 (2006.01) C07K 14/165 (2006.01)  
A61K 47/64 (2017.01) C12N 7/00 (2006.01)

(21) International Application Number:

PCT/US2017/062354

(22) International Filing Date:

17 November 2017 (17.11.2017)

(25) Filing Language:

English

(26) Publication Language:

English

(30) Priority Data:

62/424,309 18 November 2016 (18.11.2016) US

(71) Applicant: **NEW YORK BLOOD CENTER, INC.**  
[US/US]; 310 East 67th Street, New York, New York 10065 (US).

(72) Inventors: **DU, Lanying**; 64-34 102nd Street, Apt. 11X, Rego Park, New York 11374 (US). **LI, Fang**; 1063 Sherren Street West, Roseville, Minnesota 55113 (US). **JIANG, Shibo**; 144-80 Sanford Avenue, Apt. 4A, Flushing, New York 11355 (US). **ZHOU, Yusen**; Bldg. 25, Rm 1104, Dong Da Jie Street, Fengtai District, Beijing 100071 (CN).

(74) Agent: **CULLMAN, Louis C.** et al.; K&L Gates LLP, 1 Park Plaza, Twelfth Floor, Irvine, California 92614 (US).

(81) Designated States (unless otherwise indicated, for every kind of national protection available): AE, AG, AL, AM, AO, AT, AU, AZ, BA, BB, BG, BH, BN, BR, BW, BY, BZ, CA, CH, CL, CN, CO, CR, CU, CZ, DE, DJ, DK, DM, DO, DZ, EC, EE, EG, ES, FI, GB, GD, GE, GH, GM, GT, HN,

HR, HU, ID, IL, IN, IR, IS, JO, JP, KE, KG, KH, KN, KP, KR, KW, KZ, LA, LC, LK, LR, LS, LU, LY, MA, MD, ME, MG, MK, MN, MW, MX, MY, MZ, NA, NG, NI, NO, NZ, OM, PA, PE, PG, PH, PL, PT, QA, RO, RS, RU, RW, SA, SC, SD, SE, SG, SK, SL, SM, ST, SV, SY, TH, TJ, TM, TN, TR, TT, TZ, UA, UG, US, UZ, VC, VN, ZA, ZM, ZW.

(84) Designated States (unless otherwise indicated, for every kind of regional protection available): ARIPO (BW, GH, GM, KE, LR, LS, MW, MZ, NA, RW, SD, SL, ST, SZ, TZ, UG, ZM, ZW), Eurasian (AM, AZ, BY, KG, KZ, RU, TJ, TM), European (AL, AT, BE, BG, CH, CY, CZ, DE, DK, EE, ES, FI, FR, GB, GR, HR, HU, IE, IS, IT, LT, LU, LV, MC, MK, MT, NL, NO, PL, PT, RO, RS, SE, SI, SK, SM, TR), OAPI (BF, BJ, CF, CG, CI, CM, GA, GN, GQ, GW, KM, ML, MR, NE, SN, TD, TG).

Published:

- with international search report (Art. 21(3))
- with sequence listing part of description (Rule 5.2(a))

(54) Title: IMMUNOGENIC COMPOSITION FOR MERS CORONAVIRUS INFECTION

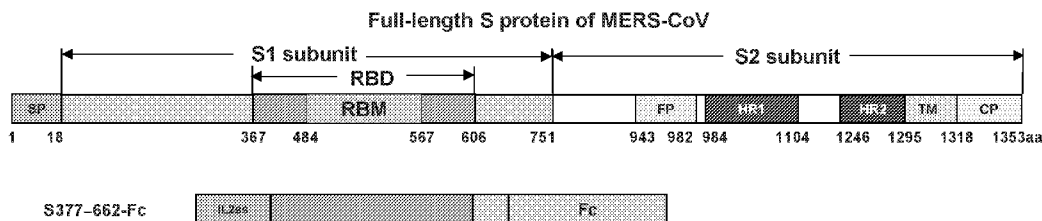


FIG. 1

(57) Abstract: Described herein are immunogenic compositions for preventing infection with Middle East respiratory syndrome coronavirus (MERS-CoV) wherein the immunogenic compositions comprise at least a portion of the MERS-CoV S protein and an immunopotentiator.



**IMMUNOGENIC COMPOSITION FOR MERS CORONAVIRUS INFECTION****CROSS REFERENCE TO RELATED APPLICATIONS**

**[0001]** The present application claims the benefit under 35 U.S.C. §119(e) to U.S. provisional patent application 62/424,309 filed November 18, 2016. The present application is also a continuation-in-part of U.S. patent application 14/375,083 filed July 28, 2014. The entire contents of both of these applications are incorporated by reference herein.

**GOVERNMENT SUPPORT CLAUSE**

**[0002]** This invention was made with government support under Grant Numbers AI089728, AI110700, AI060699, AI098775, AI124260, AI109094, AI113206 awarded by the National Institutes of Health. The Government has certain rights in the invention.

**FIELD OF THE INVENTION**

**[0003]** The present disclosure relates to the field of immunogenic compositions for the prevention and treatment of infection with human MERS coronavirus.

**BACKGROUND**

**[0004]** Coronaviruses infect and cause disease in a wide variety of species, including bats, birds, cats, dogs, pigs, mice, horses, whales, and humans. Bats act as a natural reservoir for coronaviruses. Most infections caused by human coronaviruses are relatively mild. However, the outbreak of severe acute respiratory syndrome (SARS) caused by SARS-CoV in 2002-2003, and fatal infection in 2012 caused by a recently identified coronavirus, Middle East respiratory syndrome coronavirus (MERS-CoV, also known as hCoV-EMC or NCoV) demonstrated that coronaviruses are also able to cause severe, sometimes fatal disease in humans.

**[0005]** The recently identified coronavirus MERS-CoV has over 40% mortality rate among the infected individuals. This virus also demonstrates person-to-person transmission, posing a continuous threat to public health worldwide. Thus, development of vaccines and antiviral agents against this new virus are urgently needed.

**SUMMARY**

**[0006]** Disclosed herein are immunogenic compositions for the prevention or treatment of infection with a new coronavirus MERS-CoV (also known as hCoV-EMC or NCoV). The disclosed immunogenic compositions are proteins comprising: 1) at least a portion of the MERS-CoV genome, and 2) an immunopotentiator sequence. The sequences are contiguous and expressed as a single protein in a mammalian expression system, or the MERS-CoV portion and the immunopotentiator are chemically linked and stabilized. Optionally, a stabilization sequence and/or a linker sequence are disposed between the MERS-CoV sequence and the immunopotentiator.

[0007] Also disclosed herein are immunogenic compositions comprising a protein, the protein comprising a MERS-CoV S protein sequence comprising amino acids 377-588 of the MERS-CoV S protein with a T579N mutation; and an immunopotentiator.

[0008] In one embodiment, the immunopotentiator sequence is an Fc fragment of human IgG (Fc), a C3d protein, an *Onchocerca volvulus* ASP-1, a cholera toxin, a muramyl peptide, or a cytokine. In another embodiment, the immunopotentiator is Fc.

[0009] In another embodiment, the protein further comprises a stabilization sequence disposed between the MERS-CoV S protein sequence and the immunopotentiator sequence. In another embodiment, the stabilization sequence is a foldon (Fd) or GCN4.

[0010] In yet another embodiment, the protein further comprises a linker sequence disposed between the MERS-CoV S protein sequence and the immunopotentiator sequence, and the linker is (GGGGS)<sub>n</sub>, wherein n is an integer between 0 and 8. In another embodiment, n is 1.

[0011] In another embodiment, the protein is produced in a mammalian expression system.

[0012] In another embodiment, the protein comprises the sequence of S377-588-Fc T579N (SEQ ID NO:26).

[0013] In another embodiment, the immunogenic composition further comprises an adjuvant.

[0014] Also provided is a method of inducing a protective immune response against MERS-CoV comprising administering the immunogenic composition to a subject in need thereof; wherein the immunogenic composition induces a protective immune response against challenge with MERS-CoV in the host.

[0015] In another embodiment, the immunogenic composition further comprises an adjuvant.

[0016] In one embodiment, the administering step comprises a prime immunization and at least one boost immunization. In another embodiment, the boost immunizations are administered at least twice. In another embodiment, the boost immunizations are administered weekly, every other week, monthly, or every other month. In yet another embodiment, the boost immunizations are administered weekly, every 2 weeks, every 3 weeks, every 4 weeks, every 5 weeks, every 6 weeks, every 7 weeks, every 8 weeks, every 9 weeks, every 10 weeks, every 11 weeks, or every 12 weeks.

#### **BRIEF DESCRIPTION OF THE DRAWINGS**

[0017] FIG. 1 depicts the schematic representation of spike (S) protein of Middle East respiratory syndrome coronavirus (MERS-CoV) and the recombinant S377-662-Fc (human IgG Fc) protein. The MERS-CoV S protein includes the following functional domains in the S1 and S2: signal peptide (SP), receptor-binding domain (RBD), receptor-binding motif (RBM), fusion peptide (FP), heptad repeat 1 (HR1), heptad repeat 2 (HR2), transmembrane domain (TM), and cytoplasm domain (CP).

**[0018]** FIG. 2 depicts the SDS-PAGE and Western blot analysis of the expressed protein S377-662-Fc. The protein molecular weight marker (kDa) is indicated on the left. Antisera from mice immunized with S377-662-Fc were used for Western blot analysis.

**[0019]** FIG. 3 depicts the binding of a series of severe acute respiratory syndrome (SARS) S protein-specific mAbs (1 µg/ml) to MERS-CoV S377-662-Fc protein and SARS-CoV S-RBD protein. The HA-7 mAb specific for the hemagglutinin (HA1) of H5N1 virus was used as an unrelated mAb control. The data are presented as mean A450 ± standard deviation (SD) of duplicate wells.

**[0020]** FIG. 4A and FIG. 4B depict the antibody responses and neutralization induced by MERS-CoV S377-662-Fc protein. FIG. 4A depicts binding to MERS-CoV S377-662 and SARS-CoV S-RBD proteins by antibodies in mouse sera collected 10 days post-2<sup>nd</sup> immunization. The data are presented as mean A450 ± SD of five mice per group at various dilution points. FIG. 4B depicts neutralization of the MERS-CoV virus by the same antisera as in FIG. 4A. Neutralizing antibody titers were expressed as the reciprocal of the highest dilution of sera that completely inhibited virus-induced cytopathic effect (CPE) in at least 50% of the wells (NT<sub>50</sub>), and are presented as mean ± SD from five mice per group.

**[0021]** FIG. 5 depicts mouse immunization, sample collection, and immune response detection strategy. Four groups of mice were immunized subcutaneously (s.c.) or intranasally (i.n.) with MERS-CoV S377-662-Fc protein plus Montanide ISA51 (for s.c.) or poly(I:C) (for i.n.) adjuvant, or with PBS plus the corresponding adjuvant as their respective controls. Mouse sera and lung wash were collected as indicated and analyzed for humoral and mucosal immune responses and neutralization against MERS-CoV virus.

**[0022]** FIG. 6A and FIG. 6B depict the IgG antibody responses in sera of mice immunized (s.c. and i.n.) with MERS-CoV S377-662-Fc protein. FIG. 6A depicts binding of IgG to a MERS-CoV S1 protein containing residues 18-725 of MERS-CoV S1 with a His6 tag (S1-His). Sera from 10 days post-last immunization were used for the detection, and the data are presented as mean A450 ± SD of five mice per group at various dilution points. FIG. 6B depicts the long-term IgG antibody responses using sera collected at 0, 1, 2, 3, 4, 6 months after the first immunization and 10 days post-last immunization. The data are presented as mean (IgG endpoint titers) ± SD of five mice per group.

**[0023]** FIG. 7A and FIG. 7B depict the IgG subtypes in sera of mice immunized (s.c. and i.n.) with MERS-CoV S377-662-Fc protein. Binding of IgG1 (FIG. 7A) and IgG2a (FIG. 7B) to MERS-CoV S1-His protein is shown. Sera from 10 days post-last immunization were used for the detection, and the data are presented as geometric mean titer (GMT, endpoint titers) ± SD of five mice per group. *P* < 0.001 indicates significant difference.

**[0024]** FIG. 8A and FIG. 8B depict the IgA antibody responses in lung wash and sera of mice immunized (s.c. and i.n.) with MERS-CoV S377-662-Fc protein. Binding of IgA in lung wash (1:1,000) (FIG. 8A) or sera (FIG. 8B) to MERS-CoV S1-His protein is shown. Samples from 10 days

post-last immunization were used for the detection, and the data are presented as mean A450  $\pm$  SD (lung wash) or mean (GMT endpoint titers)  $\pm$  SD (sera) of five mice per group.  $P < 0.05$  indicates significant difference.

**[0025]** FIG. 9A and FIG. 9B depict the neutralizing antibody titer against MERS-CoV infection from samples of mice immunized (s.c. and i.n.) with MERS-CoV S377-662-Fc protein. Sera (FIG. 9A) and lung wash (1:1,000 dilution in PBS during collection) (FIG. 9B) were collected at 10 days post-last immunization and analyzed for neutralization of MERS-CoV infection in Vero E6 cells. Neutralizing antibody titers were expressed as the NT<sub>50</sub>, and are presented as GMT  $\pm$  SD from five mice per group.  $P < 0.05$  indicates significant difference.

**[0026]** FIG. 10A and FIG. 10B depict a schematic representation of the S1 subunit of MERS-CoV (FIG. 10A) and recombinant proteins containing various fragments of the RBD domain of MERS-CoV S protein (FIG. 10B). Recombinant proteins S350-588-Fc, S358-588-Fc, S367-588-Fc, S367-606-Fc, and S377-588-Fc were constructed by inserting the corresponding RBD fragments into Fc of human IgG, and compared with S377-662-Fc.

**[0027]** FIG. 11A and FIG. 11B depict the SDS-PAGE (FIG. 11A) and Western blot (FIG. 11B) analysis of the expressed MERS CoV RBD-Fc proteins. The protein molecular weight marker (kDa) is indicated on the left. Antisera from mice immunized with MERS-CoV S1-His were used for Western blot analysis.

**[0028]** FIG. 12A and FIG. 12B depict the binding of the purified MERS-CoV RBD-Fc proteins to cellular receptor dipeptidyl peptidase 4 (DPP4) in Huh-7 cells by co-immunoprecipitation followed by Western blot (FIG. 12A) and soluble DPP4 (sDPP4) by ELISA (FIG. 12B). Proteins were mixed with Huh-7 cell lysates in the presence of protein A sepharose beads, and detected by Western blot using anti-DPP4 antibodies (1  $\mu$ g/ml) or antisera from mice immunized with MERS-CoV S1-His (1:1,000), respectively.

**[0029]** FIG. 13A and FIG. 13B depict IgG antibody responses in sera of mice immunized s.c. with MERS-CoV RBD-Fc proteins. MERS-CoV S1-His protein (S1-His) was used to coat the ELISA plates. Sera from 10 days post-3<sup>rd</sup> immunization were used for the detection, and the data are presented as mean A450 (FIG. 13A) or mean endpoint titers (FIG. 13B)  $\pm$  SD of five mice per group. Sera of mice injected with PBS were included as the control.  $P$  values from different groups were indicated.

**[0030]** FIG. 14 depicts the IgG subtype antibody responses by ELISA in sera of mice immunized s.c. with MERS-CoV RBD-Fc proteins. MERS-CoV S1-His protein (S1-His) was used to coat the ELISA plates. Sera from 10 days post-3<sup>rd</sup> immunization were used for the detection, and the data are presented as mean endpoint titers  $\pm$  SD of five mice per group. Sera of mice injected with PBS were included as the control.  $P$  values from different groups were indicated.

**[0031]** FIG. 15 depicts the neutralizing antibody titer of antisera from mice immunized s.c. with MERS-CoV RBD-Fc proteins against MERS-CoV infection in Vero E6 cells. Sera from 10 days post-3<sup>rd</sup> immunization were used for the assay. Neutralizing antibody titers were expressed as the NT<sub>50</sub>, and are presented as mean ± SD from five mice per group.

**[0032]** FIG. 16A and FIG. 16B depict the flow cytometry detection of inhibition of MERS-CoV RBD-Fc protein (S377-588-Fc) binding to Huh-7 cells expressing DPP4 receptor by antisera from mice immunized with S377-588-Fc protein. FIG. 16A depicts S377-588-Fc protein (black line, right) bound to Huh-7 cells (gray shade), while the control human IgG Fc protein (black line, left) did not exhibit binding activity. FIG. 16B depicts the inhibition of S377-588-Fc binding to Huh-7 cells (gray shade) by sera from mice immunized with S377-588-Fc (white line), but not by sera from the PBS control group (black line).

**[0033]** FIG. 17 depicts the conformational structure of MERS-CoV S377-588-Fc protein by cross-linker analysis. The protein was cross-linked with glutaraldehyde or left uncross-linked (w/o cross-linker), followed by Western blot detection using antisera (1:1,000) from mice immunized with MERS-CoV S1-His. The protein molecular weight marker (kDa) is indicated on the left.

**[0034]** FIG. 18 depicts the inhibition of MERS-CoV infection in Calu-3 cells by MERS-CoV S377-588-Fc protein. Human IgG Fc (hIgG-Fc) was used as the control. The CPE ranged from 0 (none), ± (<5%), 1 (5–10%), 2 (10–25%), 3 (25–50%), and 4 (>50%).

**[0035]** FIG. 19A-D. Introduction of glycan probes to MERS-CoV RBD vaccine. (FIG. 19A) Crystal structure of MERS-CoV RBD (PDB access code: 4L3N). The core structure is colored in cyan, and the receptor-binding motif (RBM) in red. Four residues are shown where an N-linked glycan probe was introduced. (FIG. 19B) Structure of MERS-CoV RBD complexed with human DPP4 (PDB access code: 4KR0), showing the role of the four epitopes in the binding of the RBD to DPP4. (FIG. 19C) AlphaScreen assay was performed to detect the binding between recombinant MERS-CoV RBDs and recombinant human DPP4. PBS buffer was used as a negative control. Binding affinity was characterized as AlphaScreen counts. Error bars indicate SEM. \*\*\*:  $P < 0.001$ . (FIG. 19D) Fluorescence-activated cell sorting (FACS) was carried out to detect the binding between recombinant MERS-CoV RBDs and cell-surface-expressed human DPP4. Human IgG protein was used as a negative control. Binding affinity was characterized as median fluorescence intensity (MFI). \*\*\*:  $P < 0.001$ .

**[0036]** FIG. 20A-E. Role of engineered glycan probes in RBD binding to neutralizing mAbs. (FIG. 20A-D) ELISA was carried out to detect the binding between recombinant MERS-CoV RBD fragments and neutralizing mAbs. The binding affinity was characterized as the ELISA signal at 450 nm. Each of the mAbs was serially diluted before being used in ELISA. \*\*\*:  $P < 0.001$ . (FIG. 20E) Structure of MERS-CoV RBD, showing the identified binding site of the neutralizing mAbs on the RBD.

**[0037]** FIG. 21A-C. Measurement of neutralizing immunogenicity of RBD epitopes. (FIG. 21A) Measurement of neutralizing antibody titers of mouse sera induced by wild type (WT) or glycosylation mutant RBD. The neutralizing antibody titer of RBD-induced mouse sera was characterized by its capability to inhibit MERS-CoV-induced cytopathic effect (CPE) in cell culture. To this end, serially diluted mouse sera were added to MERS-CoV-infected cells, and the neutralizing antibody titer of the sera was expressed as the reciprocal of the highest dilution of sera that completely inhibited MERS-CoV-induced CPE in at least 50% of the wells ( $NT_{50}$ ). PBS buffer was used as a negative control. \*:  $P < 0.05$ . (FIG. 21B) Calculation of NII for each epitope.  $NT_{50-wt}$  :  $NT_{50}$  for wild type RBD;  $NT_{50-probe}$  :  $NT_{50}$  for RBD containing a glycan probe on one of the epitopes. (FIG. 21C) Mapping the calculated NIIs on the three-dimensional structure of MERS-CoV RBD.

**[0038]** FIG. 22A-B. Masking negative epitope on the core led to immune refocusing on RBM. Competition assay was performed between neutralizing mAbs and glycosylation-mutant-RBD-induced mouse serum for the binding of wild type RBD. Specifically, ELISA was carried out between a neutralizing mAb, hMS-1 (FIG. 22A) or m336-Fab (FIG. 22B), and MERS-CoV RBD in the presence of mouse serum induced by the 579-glycosylated MERS-CoV RBD or mouse serum induced by the wild type MERS-CoV RBD. Mouse serum induced by PBS buffer was used as a negative control. Each of the sera was serially diluted before being used in the competition assay. For each serum dilution, the % reduction in mAb-RBD binding was computed for immune-sera present relative to immune-sera absent conditions. \*\*\*:  $P < 0.001$ .

**[0039]** FIG. 23A-B. Rational design of MERS-CoV RBD vaccine with enhanced efficacy. Mice were immunized with two engineered RBD fragments containing a glycan probe at residue 511 (R511N/E513T) and residue 579 (T579N), respectively. Wild type RBD and PBS buffer were used as controls. Immunized mice were challenged with MERS-CoV (EMC-2012 strain), and observed for survival rate (FIG. 23A) and weight changes (FIG. 23B).

#### DETAILED DESCRIPTION

**[0040]** Development of an effective and safe vaccine against a newly recognized coronavirus MERS-CoV (also known as hCoV-EMC or NCoV) is urgently needed for the prevention of current spread and future outbreaks. The present disclosure describes the development of a MERS-CoV immunogenic composition based on the spike (S) protein of MERS-CoV. This immunogenic composition induced strong immune responses and potent neutralizing antibodies in immunized animals.

**[0041]** As used herein the term "immunogen" refers to any substrate that elicits an immune response in a host. As used herein an "immunogenic composition" refers to an expressed protein or a recombinant vector, with or without an adjuvant, which expresses and/or secretes an immunogen *in vivo* and wherein the immunogen elicits an immune response in the host. The immunogenic compositions disclosed herein may or may not be immunoprotective or therapeutic. When the immunogenic compositions may prevent, ameliorate, palliate, or eliminate disease from the host

then the immunogenic composition may also optionally be referred to as a vaccine. However, the term immunogenic composition is not intended to be limited to vaccines.

**[0042]** MERS-CoV is closely related to severe acute respiratory syndrome (SARS) coronavirus (SARS-CoV). Clinically similar to SARS, MERS-CoV infection leads to severe respiratory illness with renal failure. As the sixth coronavirus known to infect humans and the first human coronavirus in lineage C of betacoronavirus (the same lineage as BatCoV-HKU-4 and -HKU-5), MERS-CoV is closely related to SARS-CoV genetically (lineage B). Therefore, MERS-CoV has recently raised serious concerns of a potential pandemic and, as such, it poses a continuous threat to public health worldwide. Human dipeptidyl peptidase 4 (DPP4) has been identified as the MERS-CoV's receptor.

**[0043]** Like other coronaviruses, the MERS-CoV virion utilizes a large surface S glycoprotein for interaction with, and entry into, the target cell. The S glycoprotein consists of a globular S1 domain at the N-terminal region, followed by membrane-proximal S2 domain, a transmembrane domain, and an intracellular domain.

**[0044]** The receptor-binding domain (RBD) of SARS-CoV S protein contains a critical neutralizing domain (CND), which induces potent neutralizing antibodies and protection against SARS-CoV infection in animal models. By comparing and analyzing the S protein sequences of MERS-CoV and SARS-CoV, it was found that the S1 subunit encompassing residues 377-662 of MERS-CoV S protein exhibited a core structure very similar to that of SARS-CoV S protein, suggesting that this region of MERS-CoV S protein also serves as a neutralizing domain. Indeed, a recombinant protein containing residues 377-662 of MERS-CoV S fused to Fc (fragment, crystallizable) domain of human IgG (S377-662-Fc, FIG. 1) was expressed in a mammalian cell expression system (FIG. 2) and is able to induce neutralizing antibodies through both subcutaneous (s.c.) and intranasal (i.n.) routes of administration in an established mouse model of MERS-CoV (FIG. 9). Additionally, recombinant RBD protein fragments spanning residues 350-606 of MERS-CoV S protein were fused to the Fc domain of human IgG (e.g., S350-588-Fc, S358-588-Fc, S367-588-Fc, S377-588-Fc, S367-606-Fc), were expressed in the mammalian cell expression system (FIG. 11), and elicited neutralizing antibodies in immunized mice (FIG. 15). Particularly, a truncated RBD region containing residues 377-588 of MERS-CoV S protein fused to Fc of human IgG (S377-588-Fc) induced a potent neutralizing antibody response in immunized mice (FIG. 15). Antisera from mice immunized with this protein effectively blocked the RBD protein binding to MERS-CoV's receptor DPP4 (FIG. 16). Furthermore, the S377-588-Fc protein was able to form dimeric or tetrameric conformational structures (FIG. 17), and effectively inhibited MERS-CoV infection in DPP4-expressing Calu-3 cells (FIG. 18).

**[0045]** In one embodiment, the S protein sequence component of the instant immunogenic composition comprises a MERS-CoV S protein sequence, a MERS-CoV S1 protein sequence, a MERS-CoV S2 protein sequence, an RBD sequence of a MERS-CoV S protein, a fusion sequence of a MERS-CoV S protein, a heptad repeat sequence of a MERS-CoV S protein, a nucleocapsid



sequence of a MERS-CoV S protein, a membrane sequence of a MERS-CoV S protein, or a portion of any of these sequences. In one embodiment, the S protein sequence comprises amino acids 377-662 (SEQ ID NO:2), 377-588 (SEQ ID NO:3), 350-588 (SEQ ID NO:4), 358-588 (SEQ ID NO:5), 367-588 (SEQ ID NO:6), or 367-606 (SEQ ID NO:7) of MERS-CoV S protein.

**Table 1.** Amino acid sequences of MERS-CoV regions and immunopotentiators

SEQ ID NO.1 [MERS-CoV S protein]:

MIHSVFLLMFLLTPTESYVDVGPDSVKSACIEVDIQQTFDFKTWPRPIDVSKADGIYPQGRITYSNITI  
 TYQGLFPYQGDHGDYVYSAGHATGTPPQKLFVANYSQDVKQFANGFVVRIGAAANSTGTVIISPS  
 TSATIRKIYPAFMLGSSVGNFSDGKMGRRFFNHTLVLLPDGCGTLLRAFYCILEPRSGNHCPAGNSYT  
 SFATYHTPATDCSDGNYNRNASLNSFKEYFNLRNCTFMYYTINITEDEILEWFGITQTAQGVHLFSSR  
 YVDLYGGNMFQFATLPVYDTIKYYSIIPHSIRSIQSDRKAWAAFVYVYKQLPLTFLLDFSDGYIRRAID  
 CGFNDLSQLHCSYESFDVESGVYSVSSFEAKPSGSVVEQAEGVECDFSPLLSGTPPQVYNFKRLV  
 FTNCNYNLTKLLSLFSVNDFTCSQISPAAIASNCYSSLILDYFSYPLSMKSDLSVSSAGPISQFNKQ  
 SFSNPTCLILATVPHNLTTITKPLKYSYINKCSRLLSDDRTEVPQLVNANQYSPCVSIVPSTVWEDGD  
 YYRKQLSPLEGGGWLVASGSTVAMTEQLQMGFGITVQYGTDTNSVCPKLEFANDTKIASQLGNCV  
 EYSLYGVSGRQVFQVAVGVRQRFVYDAYQNLVGYYSDDGNYCLRACVSVVSVIYDKETKT  
 HATLFGSVACEHISSTMSQYSRSTRSMLKRRDSTYGPLQTPVGCVLGLVNSSLFVEDCKLPLGQSL  
 CALPDTPTLTPRSVRSVPGEMRLASIAFNHPIQVDQLNSSFYKLSIPTNFSFGVTQEYIQTITQKVT  
 VDCKQYVCNGFQKCEQLLREYGFQFCSKINQALHGANLRQDDSVRNLFASVKSSQSSPIIPGFGGD  
 FNLTLLPVSISTGSRARSARSAIEDLLFDKVTIADPGYMQGYDDCMQQGPASARDLICAQYVAGYKVL  
 PPLMDVNMEAAAYTSSLLGSIAGVGTAGLSSFAAIPFAQSIFYRLNGVGITQQVLSQKLIANKFN  
 QALGAMQTGFTTTNEAFQKVQDAVNNAQALSKLASELSNTFGAISASIGDIIQRDLVLEQDAQIDR  
 LINGRLTTLNFAVQQLVRSESAALSAQLAKDKVNECVKAQSKRSGFCGQGTHIVSFVNAPNGLY  
 FMHVGYPSNHIEVVSAYGLCDAANPTNCIAPVNGYFIKTNTRIVDEWSYTGSSFYAPEPITSLNT  
 KYVAPQVTYQNIQNLPPPLGNSTGIDFQDELDEFFKNVSTSIPIFGSLTQINTLLDLTYEMLSLQ  
 QVVKALNESYIDLKELGNYTYNKWPWYIWLGFIAGLVALALCVFFILCCTGCGTNCMGKLCNRC  
 CDRYEEYDLEPHKVHVH

SEQ ID NO.2 [aa377-662 of MERS-CoV S protein]:

QAEGVECDFSPLLSGTPPQVYNFKRLVFTNCNYNLTKLLSLFSVNDFTCSQISPAAIASNCYSSLILD  
 YFSYPLSMKSDLSVSSAGPISQFNKQSFNSNPTCLILATVPHNLTTITKPLKYSYINKCSRLLSDDRTE  
 VPQLVNANQYSPCVSIVPSTVWEDGDYYRKQLSPLEGGGWLVASGSTVAMTEQLQMGFGITVQY  
 GTDTNSVCPKLEFANDTKIASQLGNCVEYSLYGVSGRQVFQVAVGVRQRFVYDAYQNLVGYYS  
 SDDGNYCLRACVSVVSVI

SEQ ID NO.3 [aa377-588 of MERS-CoV S protein]:

QAEGVECDFSPLLSGTPPQVYNFKRLVFTNCNYNLTKLLSLFSVNDFTCSQISPAAIASNCYSSLILD  
 YFSYPLSMKSDLSVSSAGPISQFNKQSFNSNPTCLILATVPHNLTTITKPLKYSYINKCSRLLSDDRTE  
 VPQLVNANQYSPCVSIVPSTVWEDGDYYRKQLSPLEGGGWLVASGSTVAMTEQLQMGFGITVQY  
 GTDTNSVCPKL

SEQ ID NO.4 [aa350-588 of MERS-CoV S protein]:

SYESFDVESGVYSVSSFEAKPSGSVVEQAEGVECDFSPLLSGTPPQVYNFKRLVFTNCNYNLTKLL  
 SLFSVNDFTCSQISPAAIASNCYSSLILDYFSYPLSMKSDLSVSSAGPISQFNKQSFNSNPTCLILATV  
 PHNLTTITKPLKYSYINKCSRLLSDDRTEVPQLVNANQYSPCVSIVPSTVWEDGDYYRKQLSPLEGG  
 GWLVASGSTVAMTEQLQMGFGITVQYGTDTNSVCPKL

SEQ ID NO.5 [aa358-588 of MERS-CoV S protein]:

SGVYSVSSFEAKPSGSVVEQAEGVECDFSPLLSGTPPQVYNFKRLVFTNCNYNLTKLLSLFSVNDFT  
 TCSQISPAAIASNCYSSLILDYFSYPLSMKSDLSVSSAGPISQFNKQSFNSNPTCLILATVPHNLTTITK  
 PLKYSYINKCSRLLSDDRTEVPQLVNANQYSPCVSIVPSTVWEDGDYYRKQLSPLEGGGWLVASG  
 STVAMTEQLQMGFGITVQYGTDTNSVCPKL

SEQ ID NO.6 [aa367-588 of MERS-CoV S protein]:

EAKPSGSVVEQAEGVECDFSPLLSGTPPQVYNFKRLVFTNCNYNLTKLLSLFSVNDFTCSQISPAAI  
ASNCYSSLILDYFSYPLSMKSDLSVSSAGPISQFNFKQSFNSPTCLILATVPHNLTTITKPLKYSYINK  
CSRLSDDRTEVPQLVNANQYSPCVSIVPSTVWEDGDYRQKQLSPLEGGGWLVASGSTVAMTEQL  
QMFGGITVQYGTDTNSVCPKL

SEQ ID NO.7 [aa367-606 of MERS-CoV S protein]:

EAKPSGSVVEQAEGVECDFSPLLSGTPPQVYNFKRLVFTNCNYNLTKLLSLFSVNDFTCSQISPAAI  
ASNCYSSLILDYFSYPLSMKSDLSVSSAGPISQFNFKQSFNSPTCLILATVPHNLTTITKPLKYSYINK  
CSRLSDDRTEVPQLVNANQYSPCVSIVPSTVWEDGDYRQKQLSPLEGGGWLVASGSTVAMTEQL  
QMFGGITVQYGTDTNSVCPKLEFANDTKIASQLGNCVEY

SEQ ID NO.8 [S350-588-Fc]:

SYESFDVESGVYSVSSFEAKPSGSVVEQAEGVECDFSPLLSGTPPQVYNFKRLVFTNCNYNLTKLL  
SLFSVNDFTCSQISPAAIASNCYSSLILDYFSYPLSMKSDLSVSSAGPISQFNFKQSFNSPTCLILATV  
PHNLTTITKPLKYSYINKCSRLSDDRTEVPQLVNANQYSPCVSIVPSTVWEDGDYRQKQLSPLEGG  
GWLVASGSTVAMTEQLQMFGGITVQYGTDTNSVCPKLRSDKTHTCPPCPAPELLGGPSVFLFPPK  
PKDTLMISRTPPEVTCVVDVSHEDPEVKFNWYVDGVEVHNAKTKPREEQYNSTYRWSVLTVLHQ  
DWLNGKEYKCKVSNKALPAPIEKTISKAKGQPREPQVYTLPPSREEMTKNQVSLTCLVKGFYPSDIA  
VEWESNGQPENNYKTTPVLDSDGSFFLYSKLTVDKSRWQQGNVFCSSVMHEALHNHYTQKSLS  
LSPGK

SEQ ID NO.9 [S358-588-Fc]:

SGVYSVSSFEAKPSGSVVEQAEGVECDFSPLLSGTPPQVYNFKRLVFTNCNYNLTKLLSLFSVNDF  
TCSQISPAAIASNCYSSLILDYFSYPLSMKSDLSVSSAGPISQFNFKQSFNSPTCLILATVPHNLTTITK  
PLKYSYINKCSRLSDDRTEVPQLVNANQYSPCVSIVPSTVWEDGDYRQKQLSPLEGGGWLVASG  
STVAMTEQLQMFGGITVQYGTDTNSVCPKLRSDKTHTCPPCPAPELLGGPSVFLFPPKPKDTLMIS  
RTPEVTCVVDVSHEDPEVKFNWYVDGVEVHNAKTKPREEQYNSTYRWSVLTVLHQDWLNGKE  
YKCKVSNKALPAPIEKTISKAKGQPREPQVYTLPPSREEMTKNQVSLTCLVKGFYPSDIAVEWESN  
GQPENNYKTTPVLDSDGSFFLYSKLTVDKSRWQQGNVFCSSVMHEALHNHYTQKSLSLSPGK

SEQ ID NO.10 [S367-588-Fc]:

EAKPSGSVVEQAEGVECDFSPLLSGTPPQVYNFKRLVFTNCNYNLTKLLSLFSVNDFTCSQISPAAI  
ASNCYSSLILDYFSYPLSMKSDLSVSSAGPISQFNFKQSFNSPTCLILATVPHNLTTITKPLKYSYINK  
CSRLSDDRTEVPQLVNANQYSPCVSIVPSTVWEDGDYRQKQLSPLEGGGWLVASGSTVAMTEQL  
QMFGGITVQYGTDTNSVCPKLRSDKTHTCPPCPAPELLGGPSVFLFPPKPKDTLMISRTPPEVTCV  
VDVSHEDPEVKFNWYVDGVEVHNAKTKPREEQYNSTYRWSVLTVLHQDWLNGKEYKCKVSNKA  
LPAPIEKTISKAKGQPREPQVYTLPPSREEMTKNQVSLTCLVKGFYPSDIAVEWESNGQPENNYKT  
TPVLDSDGSFFLYSKLTVDKSRWQQGNVFCSSVMHEALHNHYTQKSLSLSPGK

SEQ ID NO.11 [S367-606-Fc]:

EAKPSGSVVEQAEGVECDFSPLLSGTPPQVYNFKRLVFTNCNYNLTKLLSLFSVNDFTCSQISPAAI  
ASNCYSSLILDYFSYPLSMKSDLSVSSAGPISQFNFKQSFNSPTCLILATVPHNLTTITKPLKYSYINK  
CSRLSDDRTEVPQLVNANQYSPCVSIVPSTVWEDGDYRQKQLSPLEGGGWLVASGSTVAMTEQL  
QMFGGITVQYGTDTNSVCPKLEFANDTKIASQLGNCVEYRSDKTHTCPPCPAPELLGGPSVFLFPP  
KPKDTLMISRTPPEVTCVVDVSHEDPEVKFNWYVDGVEVHNAKTKPREEQYNSTYRWSVLTVLH  
QDWLNGKEYKCKVSNKALPAPIEKTISKAKGQPREPQVYTLPPSREEMTKNQVSLTCLVKGFYPSD  
IAVEWESNGQPENNYKTTPVLDSDGSFFLYSKLTVDKSRWQQGNVFCSSVMHEALHNHYTQKSLS  
LSPGK

SEQ ID NO.12 [S377-588-Fc]:

QAEGVECDFSPLLSGTPPQVYNFKRLVFTNCNYNLTKLLSLFSVNDFTCSQISPAAIASNCYSSLILD  
YFSYPLSMKSDLSVSSAGPISQFNFKQSFNSPTCLILATVPHNLTTITKPLKYSYINKCSRLSDDRTE  
VPQLVNANQYSPCVSIVPSTVWEDGDYRQKQLSPLEGGGWLVASGSTVAMTEQLQMFGGITVQY  
GTDTNSVCPKLRSDKTHTCPPCPAPELLGGPSVFLFPPKPKDTLMISRTPPEVTCVVDVSHEDPEV  
KFNWYVDGVEVHNAKTKPREEQYNSTYRWSVLTVLHQDWLNGKEYKCKVSNKALPAPIEKTISKA

KGQPREPQVYTLPPSREEMTKNQVSLTCLVKGFYPSDIAVEWESNGQPENNYKTTTPVLDSGDGSF  
FLYSKLTVDKSRWQQGNVFSCSVMHEALHNHYTQKSLSLSPGK

SEQ ID NO.13 [S377-662-Fc]:

QAEGVECDFSPLLSGTPPQVYNFKRLVFTNCNYNLTKLLSLFSVNDFTCSQISPAAIASNCYSSLILD  
YFSYPLSMKSDLSVSSAGPISQFNKQSFNSPTCLILATVPHNLTTITKPLKYSYINKCSRLLSDDRTE  
VPQLVNANQYSPCVSIVPSTVWEDGDYRQKQLSPLEGGGWLVASGSTVAMTEQLQMFGGITVQY  
GTDNTNSVCPKLEFANDTKIASQLGNCVEYSLYGVSGRGVFNCTAVGVRQRFVYDAYQNLVGY  
SDDGNYCLRACVSPVSVIRSDKHTCPCPAPELLGGPSVFLFPPKPKDTLMISRTPEVTC  
VVVDVSHEDPEVKFNWYVDGVEVHNAKTKPREEQYNSTYRVVSVLTVLHQDWLNGKEYK  
CKVSNKALPAPIEKTISKAKGQPREPQVYTLPPSREEMTKNQVSLTCLVKGFYPSDIAVEW  
ESNGQPENNYKTTTPVLDSGDGSFFLYSKLTVDKSRWQQGNVFSCSVMHEALHNHYTQKS  
LSLSPGK

SEQ ID NO. 14 [Foldon (Fd)]:

GYIPEAPRDGQAYVRKDGWLLSTFL

SEQ ID NO. 15 [human IgG Fc (hFc)]:

RSDKTHTCPCPAPELLGGPSVFLFPPKPKDTLMISRTPEVTCVVVDVSHEDPEVKFNWYVDGVEV  
HNAKTKPREEQYNSTYRVVSVLTVLHQDWLNGKEYKCKVSNKALPAPIEKTISKAKGQPREPQVY  
LPPSREEMTKNQVSLTCLVKGFYPSDIAVEWESNGQPENNYKTTTPVLDSGDGSFFLYSKLTVDKSR  
WQQGNVFSCSVMHEALHNHYTQKSLSLSPGK

SEQ ID NO. 16 [mouse IgG Fc (mFc)]:

RSPRGPTIKPCPPCKCPAPNLLGGPSVFIFPPKIKDVLMSISPIVTCVVVDVSEDDPDVQISWVFN  
VEVHTAQTQTHREDYNSTLRVVSALPIQHQDWMSGKEFKCKVNNKDLPAPIERTISKPKGSVRAPQ  
VYVLPPEEEMTKKQVTLTCMVTDFMPEDIYVEWTNNGKTELNYKNTEPVLDSGDGSYFMYSKLRV  
EKKNWVERNSYSCSVHEGLHNHHTTKSFSRTPGK

SEQ ID NO. 17 [rabbit IgG Fc (rFc)]:

RSSKPTCPPPELLGGPSVFIFPPKPKDTLMISRTPEVTCVVVDVSDDDPEVQFTWYINNEQVRTAR  
PPLREQQFNSTIRVSTLPIAHQDWLRGKEFKCKVHNKALPAPIEKTISKARGQPLEPKVYTMGPPR  
EELSSRSVSLTCMINGFYPSDISVEWEKNGKAEDNYKTTPAVLDSGDGSYFLYSKLSVPTSEWQRGD  
VFTCSVMHEALHNHYTQKSISRSPGK

SEQ ID NO.18 [Human C3d (aa residues 1002–1303 in C3)]:

HLIVTPSGCGEQNMIGMTPTVIAVHYLDETEQWEKFGLEKRQGALELIKGYTQQLAFRQPSSAFA  
AFVKRAPSTWL TAYVVKVFLAVNLIADSQVLCGAVKWLILEKQKPDGVFQEDAPVIHQEMIGGLR  
NNNEKDMALTAFVLISLQEAKDICEEQVNSLPGSITKAGDFLEANYMNLQRSYTVAIAGYALAQMGR  
LKGPLLNKFLTTAKDKNRWEDPGKQLYNVEATSYALLALLQLKDFDFVPPVVRWLNEQRYGGGY  
GSTQATFMVFQALAQYQKDAPDHQELNLDVSLQLPSR

SEQ ID NO.19 [Cholera toxin b subunit (aa residues 1-124)]:

MTPQNITDLCAEYHNTQIHTLNDKIFSYTESLAGKREMAITFKNGATFQVEVPGSQHIDSQKKAIER  
MKDTRLRIAYL TEAKVEKLCVWNNKTPRAIAAISMAN

SEQ ID NO.25 [aa377-588 of MERS-CoV S protein with T579N mutation]:

QAEGVECDFSPLLSGTPPQVYNFKRLVFTNCNYNLTKLLSLFSVNDFTCSQISPAAIASNCYSSLILD  
YFSYPLSMKSDLSVSSAGPISQFNKQSFNSPTCLILATVPHNLTTITKPLKYSYINKCSRLLSDDRTE  
VPQLVNANQYSPCVSIVPSTVWEDGDYRQKQLSPLEGGGWLVASGSTVAMTEQLQMFGGITVQY  
GNDTNSVCPKL

SEQ ID NO.26 [S377-588-Fc with T579N mutation]:

QAEGVECDFSPLLSGTPPQVYNFKRLVFTNCNYNLTKLLSLFSVNDFTCSQISPAAIASNCYSSLILD  
YFSYPLSMKSDLSVSSAGPISQFNKQSFNSPTCLILATVPHNLTTITKPLKYSYINKCSRLLSDDRTE  
VPQLVNANQYSPCVSIVPSTVWEDGDYRQKQLSPLEGGGWLVASGSTVAMTEQLQMFGGITVQY  
GNDTNSVCPKL RSDKTHTCPCPAPELLGGPSVFLFPPKPKDTLMISRTPEVTCVVVDVSHEDPEV  
KFNWYVDGVEVHNAKTKPREEQYNSTYRVVSVLTVLHQDWLNGKEYKCKVSNKALPAPIEKTISKA

KGQPREPQVYTLPPSREEMTKNQVSLTCLVKGFYPSDIAVEWESNGQPENNYKTTTPVLDSDGSF  
FLYSKLTVDKSRWQQGNVFCFSVMHEALHNHYTQKSLSLSPGK

**[0046]** Optionally, a trimerization stabilization sequence is disposed between the MERS-CoV sequence and the immunopotentiator. In one embodiment, the stabilization sequence comprises a sequence that stabilizes the RGB protein sequence in a trimer or oligomer configuration. As used herein, the terms stabilization sequence, trimeric motif, and trimerization sequence are interchangeable and equivalent. Suitable stabilization sequences include, but are not limited to, a 27 amino acid region of the C-terminal domain of T4 fibrin (a foldon-like sequence) (GYIPEAPRDGQAYVRKDGEWLLSTFL, SEQ ID NO. 14 or GSGYIPEAPRDGQAYVRKDGEWLLSTFL, SEQ ID NO. 20), a GCN4 (MKQIEDKIEEILSKIYHIENEIARIKKLIGEV; SEQ ID NO. 21), an IQ (RMKQIEDKIEEIESKQKKIENEIARIKK; SEQ ID NO. 22), or an IZ (IKKEIEAIKKEQEAIKKKIEAIEK; SEQ ID NO. 23). Other suitable stabilization methods include, but are not limited to, 2,2-bipyridine-5-carboxylic acid (BPY), disulfide bonds and facile ligation.

**[0047]** In another embodiment, the immunopotentiator comprises a sequence to enhance the immunogenicity of the immunogenic composition. Suitable immunopotentiators include, but are not limited to, an Fc fragment of human IgG, a C3d (a complement fragment that promotes antibody formation binding to antigens enhancing their uptake by dendritic cells and B cells) (SEQ ID NO:18), an Ov ASP-1 (*Onchocerca volvulus* homologue of the activation associated secreted gene family) (see US 20060039921, which is incorporated by reference herein for all it discloses regarding ASP-1 adjuvants), a cholera toxin (SEQ ID NO:19), a muramyl peptide, and a cytokine.

**[0048]** In one embodiment, the immunopotentiator is an immunoglobulin Fc fragment. The immunoglobulin molecule consists of two light (L) chains and two heavy (H) chains held together by disulfide bonds such that the chains form a Y shape. The base of the Y (carboxyl terminus of the heavy chain) plays a role in modulating immune cell activity. This region is called the Fc region, and is composed of two heavy chains that contribute two or three constant domains depending on the class of the antibody. By binding to specific proteins, the Fc region ensures that each antibody generates an appropriate immune response for a given antigen. The Fc region also binds to various cell receptors, such as Fc receptors, and other immune molecules, such as complement proteins. By doing this, it mediates different physiological effects including opsonization, cell lysis, and degranulation of mast cells, basophils, and eosinophils.

**[0049]** Exemplary subunit MERS-CoV immunogenic compositions are found in FIG. 1. In certain embodiments, the coronavirus and immunopotentiator portions of the fusion protein are linked through a flexible linker comprising (GGGGS)<sub>n</sub> (SEQ ID NO:24), wherein n is an integer between 0 and 8. In certain embodiments, n is 0, n is 1, n is 2, n is 3, n is 4, n is 5, n is 6, n is 7, or n is 8.

**[0050]** The disclosed MERS-CoV immunogenic compositions include conservative variants of the proteins. A conservative variant refers to a peptide or protein that has at least one amino acid substituted by another amino acid, or an amino acid analog, that has at least one property similar to that of the original amino acid from an exemplary reference peptide. Examples of properties include, without limitation, similar size, topography, charge, hydrophobicity, hydrophilicity, lipophilicity, covalent-bonding capacity, hydrogen-bonding capacity, a physicochemical property, of the like, or any combination thereof. A conservative substitution can be assessed by a variety of factors, such as, e.g., the physical properties of the amino acid being substituted (Table 1) or how the original amino acid would tolerate a substitution (Table 2). The selections of which amino acid can be substituted for another amino acid in a peptide disclosed herein are known to a person of ordinary skill in the art. A conservative variant can function in substantially the same manner as the exemplary reference peptide, and can be substituted for the exemplary reference peptide in any aspect of the present specification.

**Table 1.** Amino Acid Properties

Property	Amino Acids
Aliphatic	G, A, I, L, M, P, V
Aromatic	F, H, W, Y
C-beta branched	I, V, T
Hydrophobic	C, F, I, L, M, V, W
Small polar	D, N, P
Small non-polar	A, C, G, S, T
Large polar	E, H, K, Q, R, W, Y
Large non-polar	F, I, L, M, V
Charged	D, E, H, K, R
Uncharged	C, S, T
Negative	D, E
Positive	H, K, R
Acidic	D, E
Basic	K, R
Amide	N, Q

**Table 2.** Amino Acid Substitutions

Amino Acid	Favored Substitution	Neutral Substitutions	Disfavored substitution
A	G, S, T	C, E, I, K, M, L, P, Q, R, V	D, F, H, N, Y, W
C	F, S, Y, W	A, H, I, M, L, T, V	D, E, G, K, N, P, Q, R
D	E, N	G, H, K, P, Q, R, S, T	A, C, I, L,
E	D, K, Q	A, H, N, P, R, S, T	C, F, G, I, L, M, V, W, Y
F	M, L, W, Y	C, I, V	A, D, E, G, H, K, N, P, Q, R, S, T
G	A, S	D, K, N, P, Q, R	C, E, F, H, I, L, M, T, V, W, Y
H	N, Y	C, D, E, K, Q, R, S, T, W	A, F, G, I, L, M, P, V

Amino Acid	Favored Substitution	Neutral Substitutions	Disfavored substitution
I	V, L, M	A, C, T, F, Y	D, E, G, H, K, N, P, Q, R, S, W
K	Q, E, R	A, D, G, H, M, N, P, S, T	C, F, I, L, V, W, Y
L	F, I, M, V	A, C, W, Y	D, E, G, H, K, N, P, Q, R, S, T
M	F, I, L, V	A, C, R, Q, K, T, W, Y	D, E, G, H, N, P, S
N	D, H, S	E, G, K, Q, R, T	A, C, F, I, L, M, P, V, W, Y
P	—	A, D, E, G, K, Q, R, S, T	C, F, H, I, L, M, N, V, W, Y
Q	E, K, R	A, D, G, H, M, N, P, S, T	C, F, I, L, V, W, Y
R	K, Q	A, D, E, G, H, M, N, P, S, T	C, F, I, L, V, W, Y
S	A, N, T	C, D, E, G, H, K, P, Q, R, T	F, I, L, M, V, W, Y
T	S	A, C, D, E, H, I, K, M, N, P, Q, R, V	F, G, L, W, Y
V	I, L, M	A, C, F, T, Y	D, E, G, H, K, N, P, Q, R, S, W
W	F, Y	H, L, M	A, C, D, E, G, I, K, N, P, Q, R, S, T, V
Y	F, H, W	C, I, L, M, V	A, D, E, G, K, N, P, Q, R, S, T

Matthew J. Betts and Robert, B. Russell, Amino Acid Properties and Consequences of Substitutions, pp. 289-316, In Bioinformatics for Geneticists, (eds Michael R. Barnes, Ian C. Gray, Wiley, 2003).

**[0051]** An MERS-CoV immunogenic composition can also comprise conservative variants to the disclosed proteins. In aspects of this embodiment, a conservative variant of an MERS-CoV immunogenic composition can be, for example, an amino acid sequence having at least 75%, at least 80%, at least 85%, at least 90%, at least 95%, at least 97%, at least 98%, or at least 99% amino acid sequence identity to the MERS-CoV immunogenic compositions disclosed herein. In other aspects of this embodiment, a conservative variant of an MERS-CoV immunogenic composition can be, for example, an amino acid sequence having at most 75%, at most 80%, at most 85%, at most 90%, at most 95%, at most 97%, at most 98%, or at most 99% amino acid sequence identity to the MERS-CoV immunogenic compositions disclosed herein.

**[0052]** In other embodiments, the MERS-CoV S protein sequence comprises an amino acid sequence having at least 75%, at least 80%, at least 85%, at least 90%, at least 95%, at least 97%, at least 98%, or at least 99% amino acid sequence identity to the MERS-CoV S amino acid sequences of any of SEQ ID NOs.1-7.

**[0053]** In still other embodiments, the immunopotentiator sequence comprises an amino acid sequence having at least 75%, at least 80%, at least 85%, at least 90%, at least 95%, at least 97%, at least 98%, or at least 99% amino acid sequence identity to the immunopotentiator amino acid sequences of any of SEQ ID NOs.9-11, 17 or 18.

**[0054]** In other aspects of this embodiment, a conservative variant of an MERS-CoV immunogenic composition, a MERS-CoV S protein amino acid sequence, or an immunopotentiator amino acid sequence can have, for example, 1, 2, 3, 4, 5, 6, 7, 8, 9, 10, 11, 12, 13, 14, 15, or more conservative substitutions, to the amino acid sequence of the MERS-CoV immunogenic compositions, MERS-CoV S protein, or immunopotentiator disclosed herein. In other aspects of this embodiment, a conservative variant of an MERS-CoV immunogenic composition, a MERS-CoV S protein amino acid sequence, or an immunopotentiator amino acid sequence can be, for example, an amino acid sequence having at least 1, at least 2, at least 3, at least 4, at least 5, at least 6, at least 7, at least 8, at least 9, at least 10, at least 11, at least 12, at least 13, at least 14, or at least 15 conservative substitutions to the amino acid sequence of the MERS-CoV immunogenic compositions, MERS-CoV S protein, or immunopotentiator disclosed herein. In yet other aspects of this embodiment, a conservative variant of an MERS-CoV immunogenic composition, a MERS-CoV S protein amino acid sequence, or an immunopotentiator amino acid sequence can be, for example, an amino acid sequence having at most 1, at most 2, at most 3, at most 4, at most 5, at most 6, at most 7, at most 8, at most 9, at most 10, at most 11, at most 12, at most 13, at most 14, or at most 15 conservative substitutions to the amino acid sequence of the MERS-CoV immunogenic compositions, MERS-CoV S protein, or immunopotentiator disclosed herein. In further aspects of this embodiment, a conservative variant of an MERS-CoV immunogenic composition, a MERS-CoV S protein amino acid sequence, or an immunopotentiator amino acid sequence can be, for example, an amino acid sequence having from 1 to 15, 2 to 15, 3 to 15, 4 to 15, 5 to 15, 6 to 15, 7 to 15, 1 to 12, 2 to 12, 3 to 12, 4 to 12, 5 to 12, 6 to 12, 7 to 12, 1 to 10, 2 to 10, 3 to 10, 4 to 10, 5 to 10, 6 to 10, 7 to 10, 1 to 8, 2 to 8, 3 to 8, 4 to 8, 5 to 8, 6 to 8, 1 to 6, 2 to 6, 3 to 6, 4 to 6, 1 to 4, 2 to 4, or 1 to 3 conservative substitutions to the amino acid sequence of the MERS-CoV immunogenic compositions, MERS-CoV S protein, or immunopotentiator disclosed herein.

**[0055]** Expression systems such as the following are suitable for use in expressing the disclosed fusion proteins: mammalian cell expression systems such as, but not limited to, the pcDNA and GS Gene expression systems; insect cell expression systems such as, but not limited to, Bac-to-Bac, baculovirus, and DES expression systems; and *E. coli* expression systems including, but not limited to, pET, pSUMO, and GST expression systems.

**[0056]** Various advantages are associated with expression of proteins in mammalian cell expression systems. The mammalian cell expression system is a relatively mature eukaryotic system for expression of recombinant proteins. It is more likely to achieve a correctly folded soluble protein with proper glycosylation, making the expressed protein maintain its native conformation and keep sufficient bioactivity. This system can either transiently or stably express recombinant antigens, and promote signal synthesis. Recombinant proteins expressed in this way may maintain proper antigenicity and immunogenicity. However, both insect and bacterial expression systems provide inexpensive and efficient expression of proteins, which may be appropriate under certain conditions.

**[0057]** The purification systems used to purify the recombinant proteins are dependent on whether a tag is linked or fused with the coronavirus sequence. If the fusion proteins are fused with IgG Fc, Protein A, or Protein G, affinity chromatography is used for the purification. If the fusion proteins are fused with GST proteins, the GST columns will be used for the purification. If the fusion proteins link with 6xHis tag at the N- or C- terminal, the expressed proteins are to be purified using His tag columns. If no tag is linked with the fusion protein, the expressed protein could be purified using fast protein liquid chromatography (FPLC), high performance liquid chromatography (HPLC), or other chromatography.

**[0058]** In certain embodiments, the immunogenic compositions further comprise or are administered with an adjuvant. Adjuvants suitable for use in animals include, but are not limited to, Freund's complete or incomplete adjuvants, Sigma Adjuvant System (SAS), and Ribi adjuvants. Adjuvants suitable for use in humans include, but are not limited to, MF59 (an oil-in-water emulsion adjuvant); Montanide ISA 51 or 720 (a mineral oil-based or metabolizable oil-based adjuvant); aluminum hydroxide, -phosphate, or -oxide; HAVLOGEN<sup>®</sup> (an acrylic acid polymer-based adjuvant, Intervet Inc., Millsboro, DE); polyacrylic acids; oil-in-water or water-in-oil emulsion based on, for example a mineral oil, such as BAYOL<sup>™</sup> or MARCOL<sup>™</sup> (Esso Imperial Oil Limited, Canada), or a vegetable oil such as vitamin E acetate; saponins; and *Onchocerca volvulus* activation-associated protein-1 (Ov ASP-1) (see US 20060039921, which is incorporated by reference herein for all it discloses regarding Ov ASP-1 adjuvants). However, components with adjuvant activity are widely known and, generally, any adjuvant may be utilized that does not adversely interfere with the efficacy or safety of the vaccine and/or immunogenic composition.

**[0059]** Vaccines and/or immunogenic compositions according to the various embodiments disclosed herein can be prepared and/or marketed in the form of a liquid, frozen suspension, or in a lyophilized form. Typically, vaccines and/or immunogenic compositions prepared according to the present disclosure contain a pharmaceutically acceptable carrier or diluent customarily used for such compositions. Carriers include, but are not limited to, stabilizers, preservatives, and buffers. Suitable stabilizers are, for example SPGA, Tween compositions (such as are available from A.G. Scientific, Inc., San Diego, Calif.), carbohydrates (such as sorbitol, mannitol, starch, sucrose, dextran, glutamate, or glucose), proteins (such as dried milk serum, albumin, or casein), or degradation products thereof. Examples of suitable buffers include alkali metal phosphates. Suitable preservatives include thimerosal, merthiolate, and gentamicin. Diluents include water, aqueous buffer (such as buffered saline), alcohols, and polyols (such as glycerol).

**[0060]** Also disclosed herein are methods for inducing an immune response to a MERS-CoV using the disclosed proteins. Generally, the vaccine and/or immunogenic composition may be administered subcutaneously, intradermally, submucosally, intranasally, or intramuscularly in an effective amount to prevent infection from the MERS-CoV and/or treat an infection from the MERS-CoV. An effective amount to prevent infection is an amount of immunizing protein that will induce immunity in the immunized animals against challenge by a virulent virus such that infection is



prevented or the severity is reduced. Immunity is defined herein as the induction of a significant higher level of protection in a subject after immunization compared to an unimmunized group. An effective amount to treat an infection is an amount of immunizing protein that induces an appropriate immune response against MERS-CoV such that severity of the infection is reduced.

**[0061]** Protective immune responses can include humoral immune responses and cellular immune responses. Protection against MERS-CoV is believed to be conferred through serum antibodies (humoral immune response) directed to the surface proteins, with mucosal IgA antibodies and cell-mediated immune responses also playing a role. Cellular immune responses are useful in protection against MERS-CoV virus infection with CD4+ and CD8+ T cell responses being particularly important. CD8+ immunity is of particular importance in killing virally infected cells.

**[0062]** Additionally, the disclosed proteins and/or immunogenic compositions can be administered using immunization schemes known by persons of ordinary skill in the art to induce protective immune responses. These include a single immunization or multiple immunizations in a prime-boost strategy. A boosting immunization can be administered at a time after the initial, prime, immunization that is days, weeks, months, or even years after the prime immunization. In certain embodiments, a boost immunization is administered 2 weeks, 1 month, 2 months, 3 months, 4 months, 5 months, or 6 months or more after the initial prime immunization. Additional multiple boost immunizations can be administered such as weekly, every other week, monthly, every other month, every third month, or more. In other embodiments, the boost immunization is administered every 3 weeks, every 4 weeks, every 5 weeks, every 6 weeks, every 7 weeks, every 8 weeks, every 9 weeks, every 10 weeks, every 11 weeks, or every 12 weeks. In certain embodiments, boosting immunizations can continue until a protective anti-MERS-CoV antibody titer is seen in the subject's serum. In certain embodiments, a subject is given one boost immunization, two boost immunizations, three boost immunizations, or four or more boost immunizations, as needed to obtain a protective antibody titer. In other embodiments, the adjuvant in the initial prime immunization and the adjuvant in the boost immunizations are different.

**[0063]** Further, in various formulations of the proteins and/or immunogenic compositions, suitable excipients, stabilizers, and the like may be added as are known by persons of ordinary skill in the art.

**[0064]** The disclosed proteins, immunogenic compositions, and methods may be used to prevent MERS-CoV virus infection in a subject susceptible thereto such as, but not limited to, a human, a primate, a domesticated animal, an animal in the wild, or a bird.

## EXAMPLES

Example 1**[0065]** Materials and Methods

**[0066]** *Construction, expression, and purification of recombinant proteins.* The construction, expression, and purification of the recombinant protein fused with Fc (S350-588-Fc, S358-588-Fc, S367-588-Fc, S367-606-Fc, S377-588-Fc, and S377-662-Fc) were done as follows. Briefly, genes encoding residues 350-588, 358-588, 367-588, 367-606, 377-588, or 377-662 of MERS-CoV S protein were amplified by PCR using synthesized codon-optimized MERS-CoV S sequences (GenBank: AFS88936.1) as the template. These fragments were then digested by EcoRI and BglII restriction enzymes and inserted into the pFUSE-hlgG1-Fc2 expression vector (hereinafter named Fc). The sequence-confirmed recombinant plasmids were respectively transfected into 293T cells which had been seeded 24 hr before transfection, followed by replacing culture medium with serum-free DMEM 8-10 hr later, and collection of supernatant containing expressed protein 72 hr post-transfection. The recombinant S350-588-Fc, S358-588-Fc, S367-588-Fc, S367-606-Fc, S377-588-Fc, and S377-662-Fc proteins were then purified by Protein A affinity chromatography.

**[0067]** *SDS-PAGE and Western blot.* The purified proteins were analyzed by SDS-PAGE and Western blot. Briefly, the proteins were either boiled at 95°C for 5 min or not boiled, and separated by 10% Tris-Glycine gel. The proteins were then stained with Coomassie Blue or transferred to nitrocellulose membranes for Western blot analysis. After blocking with 5% non-fat milk in PBST overnight at 4°C, the blots were incubated for 1 hr at room temperature with MERS-CoV S1-specific polyclonal antibodies (1:1,000). After three washes, the blots were then incubated with horseradish peroxidase (HRP)-conjugated goat anti-mouse IgG (1:5,000) for 1 hr at room temperature. Signals were visualized with ECL Western blot substrate reagents and Amersham Hyperfilm.

**[0068]** *Mouse immunization and sample collection.* Mice were prime-immunized s.c. with 10 µg/mouse of recombinant S350-588-Fc, S358-588-Fc, S367-588-Fc, S367-606-Fc, S377-588-Fc, or S377-662-Fc protein formulated with Montanide ISA 51 adjuvant, or i.n. with 10 µg/mouse of recombinant S377-662-Fc formulated with poly(I:C) adjuvant. Both groups were boosted with 10 µg/mouse of the same immunogen and adjuvant at 3-week intervals. Sera were collected at 10 days post-last immunization to detect MERS-CoV S1-specific IgG antibodies and neutralizing antibodies.

**[0069]** *ELISA.* Collected mouse sera were analyzed for MERS-CoV or SARS-CoV S-specific antibody responses by ELISA. Briefly, 96-well ELISA plates were respectively precoated with recombinant proteins overnight at 4°C and blocked with 2% non-fat milk for 2 hr at 37°C. Serially diluted mouse sera or monoclonal antibodies (mAbs) were added to the plates and incubated at 37°C for 1 hr, followed by four washes. Bound antibodies were incubated with HRP-conjugated goat anti-mouse IgG (1:2,000) for 1 hr at 37°C. The reaction was visualized by substrate 3,3',5,5'-

tetramethylbenzidine (TMB) and stopped by 1 N H<sub>2</sub>SO<sub>4</sub>. The absorbance at 450 nm (A<sub>450</sub>) was measured by ELISA plate reader.

**[0070]** *Live virus-based neutralization assay.* Neutralizing antibody titers of mouse sera against infection by live MERS-CoV or SARS-CoV were further detected as described below. Briefly, serial 2-fold dilutions of mouse sera or mAbs were incubated with 100 TCID<sub>50</sub> (50% tissue culture infective dose) of MERS-CoV or SARS-CoV for 1 hr at 37°C prior to addition to a monolayer of fetal rhesus monkey kidney (FRhK4) cells for SARS-CoV and Vero E6 cells for MERS-CoV in triplicate. Virus supernatant was removed and replaced with fresh medium after 1 hr of culture at 37°C. The cytopathic effect (CPE) in each well was observed daily and recorded on day 3 post-infection. The neutralizing titers of mouse antisera that completely prevented CPE in 50% of the wells (NT<sub>50</sub>) were calculated.

**[0071]** *Pseudovirus-based neutralization assay.* An MERS-CoV pseudovirus neutralization assay was also established for detection of neutralizing activity induced by MERS-CoV RBD-Fc protein-immunized mouse sera against MERS-CoV infection. Briefly, a plasmid expressing codon-optimized MERS-CoV (hCoV-EMC, GenBank: AFS88936.1) genes was cotransfected with a plasmid encoding Env-defective, luciferase-expressing HIV-1 genome (pNL4-3.luc.RE) into 293T cells to collect pseudovirus in supernatants. Pseudovirus-containing supernatant was incubated with serially diluted mouse sera at 37°C for 1 hr before adding to the target Huh-7 cells. Fresh medium was added 24 hr later, and the culture was continued for 72 hr. Cells were lysed by cell lysis buffer and transferred to 96-well luminometer plates. Luciferase substrate was added, and relative luciferase activity was determined by Ultra 384 luminometer. The neutralization of MERS-CoV S pseudovirus was presented as NT<sub>50</sub>.

**[0072]** Results

**[0073]** MERS-CoV S protein was expressed and its reactivity was tested with a variety of SARS-CoV S protein-specific monoclonal antibodies (mAbs) including 24H8, 31H12, 35B5, 33G4, 19B2, 17H9, S40, S50, S20, S38, S53, S44, and S29 (He, *et al.*, J. Immunol. 174:4908-15, 2005; He, *et al.*, Vaccine 24:5498-508, 2006, which are incorporated by reference herein for all they disclose regarding SARS-CoV S protein-specific MAbs). An antibody to the HA1 domain of influenza H5N1 virus, HA-7, was used as a control. Purified S377-662-Fc protein was expressed in soluble forms in the culture supernatant of transfected 293T cells, maintaining high expression with good purity (FIG. 2, left). This protein could be recognized by MERS-CoV S1-specific polyclonal antibodies, as detected by Western blot (FIG. 2, right). The expressed S377-662-Fc has a lower OD<sub>450</sub> value (most antibodies have an OD<sub>450</sub> value less 0.2) when tested by ELISA using S-specific SARS mAbs, with similar reactivity to the control HA-7 mAb (FIG. 3). These data suggest that S377-662-Fc is highly specific to the S protein of MERS-CoV, and that it maintains lower or no cross-reactivity with the majority of SARS-CoV S-specific mAbs.

**[0074]** Next, the ability of expressed MERS-CoV S377-662-Fc protein to induce antibody responses, particularly neutralizing antibodies, was tested, and the ability of S377-662-Fc to elicit cross-reactivity and cross-neutralizing activity with SARS-CoV was evaluated. Mice were immunized with MERS-CoV S377-662-Fc, and then mouse sera were collected for the detection. MERS-CoV S377-662-Fc induced IgG antibodies against the S protein of MERS-CoV after the 2<sup>nd</sup> dose of immunogenic composition, which was confirmed by coating of the ELISA plates with an MERS-CoV S-specific protein not fused to Fc (MERS-CoV S377-662) (FIG. 4A). The MERS-CoV S-specific antibodies have low or no reactivity with a recombinant RBD protein of SARS-CoV used in development of a subunit SARS candidate vaccine (FIG. 4A). Nevertheless, the anti-MERS-CoV-S antibodies could neutralize live MERS-CoV infection in cell cultures *in vitro*, as detected by a MERS-CoV neutralization assay (FIG. 4B). However, the ability of the MERS-CoV S-specific antibodies to neutralize live SARS-CoV infection is very low (<1:40). The above data suggest that MERS-CoV has low to no cross-reactivity and cross-neutralizing activity with SARS-CoV.

**[0075]** The systemic and mucosal immune responses induced by MERS-CoV RBD-Fc protein were further evaluated by immunizing mice with S377-662-Fc protein via the i.n. and s.c. immunization routes, and then detecting MERS-CoV S-specific IgG and IgA antibodies in immunized mouse sera and lung wash (FIG. 5). Indeed, sera from mice immunized via both administration routes could bind specifically to MERS-CoV S1-His protein, with the i.n. pathway inducing strong systemic humoral IgG antibody response similar to that of s.c. immunization (FIG. 6A). In addition, like the s.c. route, i.n. immunization with S377-662-Fc was able to stimulate long-term humoral immune responses in immunized mice through multiple boost immunizations, capable of maintaining protection for at least 6 months during the detection period (FIG. 6B). Furthermore, MERS-CoV S1-specific IgG1 (Th2-associated) and IgG2a (Th1-associated) antibody responses induced by the i.n. pathway were similar to those by the s.c. immunization ( $P > 0.05$ ), with a relatively higher level of IgG2a (Th1-associated) than IgG1 (Th2-associated) antibody against MERS-CoV S1 protein (FIG. 7), suggesting that MERS-CoV S377-662-Fc induced a slightly biased Th1-associated antibody response. Importantly, the i.n. immunization pathway induced similarly high level of IgA antibody to the s.c. route with equally strong neutralizing antibody responses against MERS-CoV in immunized mouse sera ( $P > 0.05$ ) (FIG. 8B and 9A), but with a significantly higher level of IgA antibody with neutralizing activity than the s.c. route in mouse lungs (FIG. 8A and 9B), indicating the ability of MERS-CoV S377-662-Fc protein in the induction of strong local mucosal immune response.

**[0076]** Structural analysis of MERS-CoV RBD alone or complexed with its receptor DPP4 has identified residues 367-588 or 367-606 of MERS-CoV S1 subunit as the essential RBD (FIG. 10A). To identify the CND in the RBD of MERS-CoV that potentially induces the highest neutralizing antibody response, five additional recombinant proteins were constructed based on the structure-defined RBD of MERS-CoV (FIG. 10B), and these proteins were evaluated for their receptor-binding, antibody responses, and neutralization activity in immunized animals. As shown in FIG.

11A, all five RBD-Fc proteins, namely S350-588-Fc, S358-588-Fc, S367-588-Fc, S377-588-Fc, and S367-606-Fc, were expressed in a mammalian cell expression system at similar expression levels as S377-662-Fc. These proteins are capable of forming suitable conformational structures, having the molecular weight of non-boiled proteins 1-fold higher than that of the boiled proteins, and being recognized by MERS-CoV S1-specific antibodies (FIG. 11B), suggesting the high specificity of these proteins to MERS-CoV. In addition, all proteins bound well to the cellular-associated DPP4 receptor, with two clear bands (corresponding to the size of DPP4 or respective MERS-CoV RBD-Fc monomers) being detected in protein-Huh-7 cell co-immunoprecipitated samples, which reacted strongly with anti-DPP4 and anti-MERS-CoV S1 (FIG. 12A). The ability of these MERS-CoV RBD-Fc proteins in the binding to sDPP4 is notably different, with S367-588-Fc, S358-588-Fc, and S377-588-Fc maintaining higher binding affinity than S377-662-Fc, S367-606-Fc, and S350-588-Fc. As expected, a control protein hIgG-Fc had no binding with sDPP4 (FIG. 12B). The comparison of the humoral immune response in immunized mice indicates that S367-588-Fc, S377-588-Fc, and S377-662-Fc were able to induce higher levels of IgG antibody than S350-588-Fc, S358-588-Fc, and S367-606-Fc (FIG. 13A and 13B), while S367-588-Fc potentially induced the highest titer of IgG2a subtype specific to the S1 of MERS-CoV (FIG. 14). More importantly, S377-588-Fc elicited the highest neutralizing antibody response among the tested RBD-Fc proteins against MERS-CoV infection (FIG. 15).

**[0077]** The produced MERS pseudovirus was able to efficiently infect a variety of target cells, including DPP4-expressing Huh-7, FRhK-4, MDCK, Vero, Vero E6, HEP-G2, A549, and Caco-2. The infection of MERS pseudovirus in target Huh-7 cells was significantly inhibited by antisera from mice immunized with MERS-CoV RBD-Fc proteins, such as the S377-588-Fc protein.

**[0078]** The S377-588-Fc protein was further characterized and evaluated for the potential as a therapeutic agent against MERS-CoV infection. Antisera from S377-588-Fc immunized mice can effectively block MERS-CoV RBD binding the DPP4 receptor, while control sera from PBS-immunized mice did not show any signs of inhibiting binding of S377-588 to DPP4-expressing Huh-7 cells (FIG. 16). The cross-linker analysis of the conformation of the S377-588-Fc indicates that this protein was able to form dimeric or tetrameric conformational structures (FIG. 17, left), which was confirmed by MERS-CoV S1-specific antibodies (FIG. 17, right). Importantly, the S377-588-Fc protein showed high ability to effectively inhibit MERS-CoV replication in the highly permissive human bronchial epithelial Calu-3 cells that express MERS-CoV's receptor DPP4, with the concentration as low as  $\sim 3$   $\mu\text{g/ml}$  inhibiting over 50% CPE formation caused by MERS-CoV infection (FIG. 18). These results suggest the use of S377-588-Fc as an important therapeutic agent against infections from MERS-CoV.

**[0079]** In conclusion, disclosed herein are recombinant proteins containing RBD fragments of MERS-CoV S1, a novel critical neutralizing domain of a new human coronavirus, MERS-CoV. These recombinant proteins, based on different fragments of RBD of MERS-CoV S protein linked to

human IgG Fc, induced potent neutralizing antibodies against infection by MERS-CoV. Previous studies on S protein-based SARS vaccines have revealed that the mean neutralizing antibody titers as low as 1:284 could protect vaccinated animals against SARS-CoV challenge, suggesting that the expressed recombinant MERS-CoV RBD-Fc proteins have a great potential to be developed as a safe and effective vaccine and therapeutic agent against MERS-CoV infection.

**[0080]** The current study revealed low to no cross-reactivity and cross-neutralizing activity of MERS-CoV with SARS-CoV, suggesting that MERS-CoV has different mechanisms of infection, including using different receptors to infect cells.

#### Example 2

**[0081]** Viral subunit vaccines often contain immunodominant non-neutralizing epitopes that divert host immune responses. These epitopes should be eliminated in vaccine design, but there is no reliable method for evaluating an epitope's capacity to elicit neutralizing immune responses. Here we introduce a new concept "neutralizing immunogenicity index" (NII) to evaluate an epitope's neutralizing immunogenicity. To determine the NII, we mask the epitope with a glycan probe and then assess the epitope's contribution to the vaccine's overall neutralizing immunogenicity. As proof-of-concept, we measure the NII for different epitopes on an immunogen comprised of the receptor-binding domain from MERS coronavirus (MERS-CoV). Further, we design a variant form of this vaccine by masking an epitope that has a negative NII. This engineered vaccine demonstrate significantly enhanced efficacy in protecting transgenic mice from lethal MERS-CoV challenge.

**[0082]** A major goal of viral subunit vaccine development is to rationally design immunogens that can elicit strong neutralizing immune responses in hosts. The receptor-binding domains (RBDs) of virus surface spike proteins are the prime candidates for subunit vaccine design because they contain epitopes that can trigger strong immune responses. In addition, viral RBDs play essential roles in viral infection cycles by binding to their host receptor for viral attachment. Thus, part of the host immune responses elicited by viral RBDs can target the receptor-binding region and thereby neutralize viral entry into host cells. Rational design of viral subunit vaccines aims to focus the immune responses on neutralizing epitopes through masking or deletion of immunodominant non-neutralizing epitopes.

**[0083]** A critical gap in subunit vaccine design is the lack of an effective way to evaluate an epitope's neutralizing immunogenicity (i.e., its capacity to elicit neutralizing immune responses). There have been extensive efforts to predict epitopes' immunogenicity based on the physical and chemical properties of the epitopes. However, these methods are not designed to predict epitopes' "neutralizing" immunogenicity, which holds the key for subunit vaccine design. Although some experimental methods are available to measure the neutralizing immunogenicity of linear epitopes by taking linear peptides out of the context of proteins, these methods do not work for conformational epitopes, which are prevalent on RBD-based viral vaccines.

**[0084]** RBD-based coronavirus vaccines have been extensively pursued due to the threat that coronaviruses pose to human health. Coronaviruses are enveloped and positive-stranded RNA viruses. In 2002-2003, SARS coronavirus (SARS-CoV) infected over 8000 people with ~10% fatality rate. Since 2012, MERS coronavirus (MERS-CoV) has infected about 1700 people with ~36% fatality rate. The RBDs from SARS-CoV and MERS-CoV both contain a core structure and a receptor-binding motif (RBM). Their core structures are highly similar, but their RBMs are markedly different, leading to different receptor specificity: SARS-CoV recognizes angiotensin-converting enzyme 2 (ACE2), whereas MERS-CoV recognizes dipeptidyl peptidase 4 (DPP4). Both SARS-CoV and MERS-CoV RBDs are capable of eliciting strong neutralizing antibody responses. On one hand, because of the enriched neutralizing epitopes in their RBM and their high-yield expression as recombinant proteins, coronavirus RBDs are promising subunit vaccine candidates. Moreover, because of their relatively simple structures compared to the intact spike proteins, coronavirus RBDs provide an excellent model system for structure-based subunit vaccine design. On the other hand, recently determined cryo-EM structures of coronavirus spike proteins revealed that whereas the RBM of coronavirus RBDs is accessible, large surface areas of the RBD core structure are buried in the full-length spike proteins. Thus, when these previously buried areas on the surface of the RBD core become exposed in recombinant RBD vaccines, they likely contain immunodominant non-neutralizing epitopes that divert host immune responses. Therefore, coronavirus RBDs both hold promises and present challenges for vaccine development. It is critical to evaluate the neutralizing immunogenicity of different epitopes on coronavirus RBDs, such that immunodominant neutralizing and non-neutralizing epitopes can be preserved and eliminated, respectively.

**[0085]** Materials and Methods

**[0086]** *Animals.* 6-8 week female BALB/c mice and 4-month female human-DPP4-transgenic mice were used in the study. The animal studies were carried out in strict accordance with the recommendations in the Guide for the Care and Use of Laboratory Animals of the National Institutes of Health. The animal protocols were approved by the Committee on the Ethics of Animal Experiments of the New York Blood Center (Permit Number: 194.17) and Beijing Institute of Microbiology and Epidemiology (Permit Number: PMB15-0012).

**[0087]** *Cell lines.* HEK293T (human embryonic kidney) and Vero E6 (monkey kidney) cells were obtained from American Type Culture Collection. Huh-7 (human hepatoma) cells were kindly provided by Dr. Charles M. Rice at Rockefeller University. These cell lines were cultured in Dulbecco's modified Eagle medium (DMEM) supplemented with 10% fetal bovine serum (FBS), 2mM L-glutamine, 100 units/mL penicillin, and 100 µg/mL streptomycin. Sf9 insect cells were purchased from Life Technologies Inc., and cultured in Sf-900 III SFM medium supplemented with 100 units/mL penicillin and 100 µg/mL streptomycin.

**[0088]** *Expression and purification of recombinant proteins.* The expression and purification of recombinant MERS-CoV RBD was carried out as previously described (Ma C, et al., Vaccine

32:6170-6176, 2014). Briefly, wild type (WT) RBD (residues 377-588; GenBank accession number: AFS88936.1) containing a C-terminal human IgG1 Fc tag was expressed in HEK293T cells, secreted into the cell culture supernatant, and purified by protein A affinity chromatography. Mutant RBD fragments containing engineered glycan probes were constructed via site-directed mutagenesis, and expressed and purified in the same way as the wild type RBD.

**[0089]** The expression and purification of recombinant human DPP4 was carried out as previously described (Yang Y, et al., Proc Natl Acad Sci USA 111:12516-12521, 2014). Briefly, human DPP4 ectodomain (residues 39-766; GenBank accession no. NP\_001926.2) containing an N-terminal human CD5 signal peptide and a C-terminal His6 tag was expressed in insect sf9 cells using the Bac-to-Bac expression system, secreted to cell culture medium, and purified sequentially on HiTrap nickel chelating HP column and Superdex 200 gel filtration column.

**[0090]** *SDS gel electrophoresis.* 5 µg wild type or mutant MERS-CoV RBDs were subjected to SDS gel electrophoresis under denatured condition. Protein bands were stained using Coomassie Brilliant Blue R, and image captured using myECL Imager (Life Technologies Inc.).

**[0091]** *Mass Spectrometry.* Wild type or mutant MERS-CoV RBDs at 100 µM concentration in 20 mM Tris-Cl, pH 7.4, 200 mM NaCl was ultrafiltrated with deionized water five times using an Amicon Ultra Centrifugal filter with a 10 kDa molecular weight cutoff. The desalted protein samples were subjected to MALDI-TOF Mass Spectrometry. Mass Spectrometry was performed in linear mode for molecular weight screening.

**[0092]** *AlphaScreen protein-protein binding assay.* Binding between recombinant MERS-CoV RBDs and recombinant human DPP4 was measured using an AlphaScreen assay as previously described (Ma et al., 2014). Briefly, 3 nM wild type or mutant MERS-CoV RBD with a C-terminal Fc tag was incubated with 300 nM human DPP4 with a C-terminal His6 tag at room temperature for 1 hr. AlphaScreen protein A acceptor beads and nickel chelate donor beads (PerkinElmer Life Sciences) were added to the mixture at a final concentration of 5 µg/ml each. After incubation at room temperature for 1 hr, the AlphaScreen signal was measured using an EnSpire plate reader (PerkinElmer Life Sciences), reflecting the binding affinity between the two proteins.

**[0093]** *FACS.* The binding between recombinant MERS-CoV RBDs and human DPP4 expressed on the Huh-7 cell surface was measured using fluorescence-activated cell sorting (FACS) as previously described (Du L, et al., J Virol 87:9939-9942, 2013). Briefly, Huh-7 cells were incubated with wild type or mutant MERS-CoV RBD (1.25 µg/ml) at room temperature for 30 min, followed by addition of FITC-conjugated anti-human-IgG-Fc polyclonal antibody (1:50 dilution) for 30 min. The amounts of RBD-bound Huh-7 cells were measured using flow cytometry, and the binding affinity between RBD and cell-surface DPP4 was characterized as median fluorescence intensity (MFI).

**[0094]** *Animal immunization and sample collection.* Animal immunization and sample collection were carried out as previously described (Ma et al., 2014). Briefly, BALB/c mice were



subcutaneously immunized with wild type or mutant MERS-CoV RBD (10 µg/mouse) in the presence of Montanide ISA51 adjuvant. PBS plus Montanide ISA51 was included as a negative control. Immunized mice were boosted twice with the same immunogen and adjuvant at a 3-week interval, and sera were collected 10 days after the last immunization for detection of neutralizing antibodies.

**[0095]** *ELISA.* The binding between recombinant MERS-CoV RBD and neutralizing mAbs was measured using ELISA as previously described (Du L, et al., J Virol 88:7045-7053, 2014). Briefly, ELISA plates were pre-coated with the same amount of wild type or mutant RBD (1 µg/ml) overnight at 4°C. After blocking with 2% non-fat milk at 37°C for 2 hr, serially diluted mAbs were added to the plates and incubated at 37°C for 1 hr. After washes, the plates were incubated at 37°C for 1 hr with horseradish-peroxidase-conjugated anti-human-IgG-Fab polyclonal antibody (1:5,000 dilution). Enzymatic reaction was carried out using substrate 3,3',5,5'-tetramethylbenzidine and stopped with 1N H<sub>2</sub>SO<sub>4</sub>. Absorbance at 450 nm (A450) was measured using ELISA Plate Reader.

**[0096]** The competition between neutralizing mAbs and mutant-RBD-induced mouse serum for the binding of wild type MERS-CoV RBD was carried out using ELISA as described above, except that the binding between wild type RBD and the neutralizing mAb (hMS-1 or m336-Fab at 5 µg/ml concentration) was performed in the presence of serially diluted mouse serum (T579N-RBD-induced, wild-type-RBD-induced, or PBS-induced). The RBD-mAb binding was detected by addition of horseradish-peroxidase-conjugated anti-human-IgG-Fab polyclonal antibody (1:5,000 dilution) and subsequent enzymatic reaction.

**[0097]** *Live MERS-CoV neutralization assay.* A micro-neutralization assay was carried out to test neutralizing antibodies against live MERS-CoV as previously described (Du et al., 2014). Briefly, serially diluted mouse sera were incubated at room temperature for 1 hr with ~100 infectious MERS-CoV virions (EMC-2012 strain), and were then incubated with Vero E6 cells at 37°C for 72 hr. The neutralizing capability of the mouse sera was measured by determining the presence or absence of virus-induced cytopathic effect (CPE). Neutralizing antibody titers were expressed as the reciprocal of the highest dilution of sera that completely inhibited virus-induced CPE in at least 50% of the wells (NT<sub>50</sub>).

**[0098]** *MERS-CoV challenge studies.* MERS-CoV challenge studies were carried out using human-DPP4-transgenic mice as previously described (Zhao G, et al., PLoS One 10:e0145561, 2015). Briefly, mice were intramuscularly immunized with wild type or mutant MERS-CoV RBD (5 µg/mouse) in the presence of aluminum adjuvant, and boosted once 4 weeks after the initial immunization. 12 weeks after the second immunization, mice were challenged with MERS-CoV (EMC-2012 strain, 10<sup>4</sup> TCID<sub>50</sub>), and observed for 21 days for detection of survival rate and weight changes.

**[0099]** *Statistical analyses.* In FIG. 19C-D, comparisons between WT RBD and each of the mutant RBDs in their binding to recombinant DPP4 by AlphaScreen (FIG. 19C) or to cell-surface

DPP4 by FACS (FIG. 19D) were done using two-tailed t-test (\*\*\*:  $P < 0.001$ ; 3 measurements for each RBD in FIG. 19C and 4 measurements for each RBD in FIG. 19D).

**[0100]** In FIG. 20A-D, nonlinear regression was performed using a log(inhibitor) vs. normalized response – variable slope model.  $R^2$  of curve fit is larger than 0.97 for all curves in FIG. 20A-D, except for the curve representing R511/E513 mutant RBD in FIG. 20A where  $R^2$  of curve fit is 0.194. Comparisons between WT RBD and each of the four mutant RBDs in their binding affinity to mAbs by ELISA were done using the extra sum-of-squares F test (\*\*\*:  $P < 0.001$ ; 12 different dilutions of each mAb, 4 measurements at each dilution for each mAb).

**[0101]** In FIG. 21A, comparisons between WT RBD and each of the mutant RBDs in their capacity to induce neutralizing serum in mice were done using two-tailed t-test (\*:  $P < 0.05$ ; 4 measurements for each RBD).

**[0102]** In FIG. 22, nonlinear regression was performed using a log(inhibitor) vs. normalized response – variable slope model.  $R^2$  of curve fit is larger than 0.98 for all curves in FIG. 22. Comparisons between WT-RBD-induced serum and T579N-RBD-induced serum in their inhibition of RBD/mAb binding by ELISA were done using the extra sum-of-squares F test (\*\*\*:  $P < 0.001$ ; 4 different dilutions of each serum, 4 measurements at each dilution for each serum).

**[0103]** All statistical analyses were performed using GraphPad Prism 6 software.

**[0104]** Results

**[0105]** *Introduction of glycan probes onto epitopes on MERS-CoV RBD.* To evaluate the neutralizing immunogenicity of a specific epitope on viral RBD vaccines, we can either delete or mask the epitope and then measure the corresponding changes in the vaccine's capacity to elicit neutralizing immune responses. Alanine scanning of vaccine-surface residues likely leads to changes in the vaccine's overall immunogenicity that are too subtle to be measurable using currently available experimental methods, while deletion of a whole epitope may disturb the tertiary structure of the viral RBD. Instead, in this study we chose to mask the epitope of interest using a host-cell-derived glycan probe. This approach is effective and convenient because the glycan probe can impose steric interference for the access of antibodies and immune cells to the epitope, and also because the glycan probe is unlikely to interfere with the folding and solubility of the RBD. To place the glycan probe on an epitope, we introduced the N-linked glycosylation motif, asparagine-X-threonine (where X is any amino acid other than proline), onto different epitopes on viral RBD vaccines using site-directed mutagenesis.

**[0106]** As proof-of-concept, we chose to study several epitopes on the MERS-CoV RBD vaccine. The Fc-tagged RBD fragment containing residues from 377 to 588 was selected in this study because we previously showed that this fragment is a stable and effective vaccine candidate (see Example 1). Four distinct epitopes on this MERS-CoV RBD fragment were selected based on their location on the RBD surface and their possible functional role in receptor binding: (i) Arg511

(located on a protruding loop and in the receptor-binding motif (RBM) region); (ii) Ala562 (located on a  $\beta$ -strand and in the RBM region); (iii) Val403 (located on a  $\beta$ -strand and in the core region); (iv) Thr579 (located on a protruding loop and in the core region) (FIG. 19A-B). Based on the three-dimensional protrusion index map, the epitopes containing Arg511 and Thr579 both have a high protrusion index, whereas the epitopes containing Ala562 and Val403 both have a low protrusion index.

**[0107]** We introduced a glycan probe onto each of the above four epitopes on MERS-CoV RBD. To this end, we introduced single mutations V403N, T579N and A562N to pair with the already existent Thr405, Thr581 and Thr564, respectively, to generate three N-linked glycosylation sites. We also introduced double mutations R511N/E513T to generate the fourth N-linked glycosylation site. Each of these glycosylation sites was located in an individual MERS-CoV RBD fragment. We expressed and purified each of the four mutant RBDs in mammalian cells.

**[0108]** *Characterization of RBDs containing engineered glycan probes.* To test whether each of the above four epitopes on MERS-CoV RBD was actually glycosylated, we performed both SDS gel electrophoresis and mass spectrometry. Compared with the wild type RBD, each of the mutant RBDs exhibited a slower electrophoretic mobility on the gel, consistent with additional glycosylation. Mass spectrometry revealed that the molecular weights of the mutant RBDs were ~1 to 2 kDa larger than that of the wild type RBD, which was also consistent with an introduced glycan probe in each of the mutant RBDs. For each of the purified mutant RBD samples, there was no visible presence of unglycosylated RBD on the SDS gel or the mass spectrometry spectrum. Thus, each of the four epitopes on MERS-CoV RBD had been successfully glycosylated.

**[0109]** To understand the correlation between the epitopes' role in receptor binding and their potential to be recognized by immune responses, we examined whether these engineered glycan probes on MERS-CoV RBD interfered with receptor binding. To this end, we used two alternative approaches. One approach was an AlphaScreen assay, which analyzed the interaction between recombinant RBDs and recombinant human DPP4 in solution (FIG. 19C), and the other approach was FACS, which examined the interaction between recombinant RBDs and human DPP4 expressed on the Huh-7 cell surface (FIG. 19D). The results from both assays revealed that the glycan probe located at residue 562 reduced the binding of the RBD to DPP4, the glycan probe located at residue 511 reduced the binding of the RBD to DPP4 even more, and the ones located at residues 403 and 579 had no impact on DPP4 binding. Structural analysis of the RBD/DPP4 interactions suggests that a glycan probe located at residue 511 would have serious steric clash with DPP4 binding, whereas a glycan probe located at residue 562 would have partial steric interference with DPP4 binding (FIG. 19B). Glycan probes located at residues 403 and 579 would be too far away from the receptor-binding region to have any impact on DPP4 binding. Hence, both the biochemical and structural analyses similarly elucidated the role of each of the glycan probes in the binding of the RBD to DPP4.

**[0110]** To understand the epitopes' potential to interact with neutralizing monoclonal antibodies (mAbs), we analyzed how the engineered glycan probes interfered with the binding of the RBD to different neutralizing mAbs. We used four humanized mAbs (hMS-1, m336-Fab, m337-Fab, and m338-Fab). All of these mAbs were previously shown to be highly potent in neutralizing MERS-CoV infection of human cells. ELISA between each of the RBDs and each of the mAbs demonstrated that the glycan probe located at residue 511 abolished the binding of the RBD to hMS-1 (FIG. 20A), reduced the binding of the RBD to m336-Fab and m337-Fab (FIG. 20B-C), and had no significant impact on the binding of the RBD to m338-Fab (FIG. 20D). In contrast, the glycan probes located at the other three residues, 403, 562 and 579, did not interfere with the binding of the RBD to any of the mAbs. The binding sites on the RBD for each of the mAbs were previously characterized through mutagenesis and/or structural studies. Three of the four mAbs, hMS-1, m336-Fab and m337-Fab, bind at or near the epitope containing Arg511, whereas all of the mAbs bind away from the epitopes containing Ala562, Val403, and Thr579 (FIG. 20E). Overall, among the four selected epitopes, the epitope containing Arg511 played the most important role in the binding of neutralizing mAbs, and consequently the glycan probe covering this epitope interfered most with the binding of neutralizing mAbs.

**[0111]** This study thus far has characterized the structural features, receptor binding, and neutralizing mAb binding for four selected RBD epitopes using a glycan probe strategy. Each of the glycan probes introduced to one of the RBD epitopes only interfered with the binding of DPP4 or mAbs that interact with this specific epitope, but had no impact on the binding of DPP4 or mAbs to distant epitopes. This observation suggests that each of the glycan probes only shielded the epitope where the glycan probe was attached to, but did not affect the structures of other antigenic sites. It is consistent with findings obtained in studies on another viral spike protein, respiratory syncytial (RSV) virus F protein.

**[0112]** *Measurement of neutralizing immunogenicity of RBD epitopes.* To evaluate how the glycan probes altered the neutralizing immunogenicity (that is, the capacity to induce neutralizing immune responses) of MERS-CoV RBDs, we immunized BALB/c mice with each of the four RBDs containing one of the glycan probes. Sera were collected from mice immunized with each of the RBDs, and tested for MERS-CoV-neutralizing antibodies. Compared to the wild type RBD vaccine, the RBDs containing a glycan probe at residues 579 and 511 induced significantly higher and lower neutralizing antibody titers, respectively, in mouse sera, whereas the RBDs containing a glycan probe at residues 403 and 562 failed to induce significant changes in neutralizing antibody titers in mouse sera (FIG. 21A). Thus, masking the epitope containing Arg511 led to reduced neutralizing antibody titers in the immunized mice, demonstrating that this epitope made a positive contribution to the vaccine's overall neutralizing immunogenicity. Based on the same rationale, the epitope containing Thr579 made a negative contribution and the epitopes containing Val403 and Ala562 made insignificant contributions to the vaccine's overall neutralizing immunogenicity. The

experiments were further repeated twice and similar results were obtained. These results provided a qualitative evaluation of the neutralizing immunogenicity for each of these epitopes.

**[0113]** Here we introduce a novel concept “neutralizing immunogenicity index” (NII) to describe an epitope’s neutralizing immunogenicity. NII is defined as the contribution of an epitope to the vaccine’s overall neutralizing immunogenicity. It can be determined by masking the epitope with a glycan probe and then measuring the relative change of the vaccine’s overall capacity to elicit neutralizing antibody titers (FIG. 21B). Based on this definition, we calculated the NII for each of the four epitopes on the RBD (FIG. 21C). The epitope containing Thr579 had an NII of -3.0. The negative sign of the NII suggests a negative contribution from this epitope to the vaccine’s overall neutralizing immunogenicity, and the value of the NII implicates that masking this epitope using a glycan probe increased the vaccine’s overall neutralizing immunogenicity by three-fold. Conversely, the epitope containing Arg511 had an NII of 0.6, suggesting that this epitope made a positive contribution to the vaccine’s overall neutralizing immunogenicity and that masking this epitope using a glycan probe reduced the vaccine’s overall neutralizing immunogenicity to 60% of that of the wild type vaccine. Therefore, the NII can serve as an effective tool to quantitatively evaluate the neutralizing immunogenicity of any epitope on the MERS-CoV RBD vaccine.

**[0114]** To investigate why masking a negative epitope led to enhanced neutralizing immunogenicity of the MERS-CoV RBD vaccine, we performed a competition assay between neutralizing mAbs and mutant-RBD-induced mouse serum for the binding of wild type MERS-CoV RBD. More specifically, ELISA was carried out between a neutralizing mAb and MERS-CoV RBD in the presence of mouse serum induced by the 579-glycosylated MERS-CoV RBD (FIG. 22A-B). As a comparison, the mouse serum induced by the wild type MERS-CoV RBD was also included. Two different mAbs were used in the competition binding assay: hMs-1, which binds to the RBM epitope containing Arg511, and m336-Fab, which binds to the RBM epitope surrounding Glu536-Asp539. The result showed that the serum induced by the 579-glycosylated RBD inhibited the mAb-RBD binding significantly better than the serum induced by the wild type RBD, revealing enhanced neutralizing capability of the mouse serum due to the glycosylation at the 579 position. Moreover, the mouse serum induced by the 579-glycosylated RBD demonstrated enhanced binding for at least two separate neutralizing epitopes on the RBM, one surrounding Arg511 and the other Glu536-Asp539. Thus, masking an epitope on the RBD core structure with a high negative NII refocuses the host immune response on neutralizing epitopes on the RBM, leading to enhanced neutralizing immunogenicity of the RBD vaccine.

**[0115]** *Rational design of RBD vaccine with enhanced efficacy.* To prove that highly effective MERS-CoV RBD vaccines can be rationally designed based on epitopes’ neutralizing immunogenicity, we investigated the efficacy of two engineered MERS-CoV RBD vaccines using virus challenge studies. These engineered RBD vaccines have a negative epitope (i.e., the epitope containing Thr579 and with an NII of -3.0) and a positive epitope (i.e., the epitope containing Arg511 and with an NII of 0.6) masked, respectively, by a glycan probe. We chose to mask the epitopes

rather than deleting them or mutating all of their residues to alanines because introducing a glycan is more convenient in practice and less disruptive to the immunogen's tertiary structure. The wild type RBD vaccine was used as a control. The animal model for vaccine testing was the lethal transgenic mouse model expressing human DPP4 (hDPP4-Tg mice). These mice were chosen for analysis because they are very susceptible to MERS-CoV and also because preventing disease in these mice is a stringent test of efficacy. Briefly, hDPP4-Tg mice were immunized with each of the RBD vaccines and challenged with MERS-CoV, and the survival rate and weight changes of the mice were recorded.

**[0116]** The efficacies of the RBD vaccines were evaluated based on the morbidity and mortality of the immunized and challenged mice. First, hDPP4-Tg mice immunized with the negative-epitope-masked RBD vaccine (i.e., RBD containing T579N mutation) all survived MERS-CoV challenge (100% survival rate), whereas hDPP4-Tg mice immunized with the wild type RBD vaccine and with the positive-epitope-masked RBD vaccine (i.e., RBD containing R511N/E513T mutations) demonstrated survival rates of 67% and 17%, respectively, after MERS-CoV challenge (FIG. 23A). Second, MERS-CoV challenge did not cause any weight loss in hDPP4-Tg mice immunized with the negative-epitope-masked RBD vaccine, but led to significant weight loss in hDPP4-Tg mice immunized with either the wild type RBD vaccine or the positive-epitope-masked RBD vaccine (FIG. 23B). The experiments were further repeated twice and similar results were obtained. These results revealed the enhanced efficacy of the negative-epitope-masked RBD vaccine and reduced efficacy of the positive-epitope-masked RBD vaccine, and demonstrated the utility of NII in developing a vaccine with increased immunogenicity in a stringent model of severe MERS.

**[0117]** Current vaccine design lacks an effective approach to evaluate the neutralizing immunogenicity of epitopes on viral subunit vaccines. In this study, we have developed a novel approach to measure vaccine epitopes' neutralizing immunogenicity. Using the MERS-CoV RBD as a model, we singly mask selected epitopes using host-derived glycan probes, and then measure the corresponding changes in the vaccine's overall neutralizing immunogenicity. We have also developed a method for calculating the NII for the selected epitopes. An epitope's neutralizing immunogenicity contains two parts: the neutralization capacity and immunogenicity. On the one hand, an epitope's neutralizing capacity is determined by the physical overlap of the epitope with the receptor-binding region and the potential role of the epitope in receptor binding. On the other hand, an epitope's immunogenicity is determined by its immune selfness (i.e., how similar or dissimilar the viral epitope is to a host-originated epitope), protrusion, and other physical and chemical properties of the epitope. Logically, an epitope's NII is correlated with a combination of factors such as immune selfness, protrusion, potential overlap with receptor-binding region, and more. Because of the complex nature of NII, it is unlikely that the NII can be reliably predicted by software; instead, this study demonstrates that NII can be experimentally measured using the glycan probe approach.

**[0118]** As proof-of-concept, we measured the NII for four distinct epitopes on the MERS-CoV RBD vaccine, and also characterized the protrusion index, receptor binding, and monoclonal antibody binding of the RBDs each with an epitope masked by a glycan probe. The results revealed that the epitopes with a high and low protrusion index tend to have an NII with a high and low absolute value, respectively. In addition, epitopes within the receptor-binding region tend to have a positive NII, and the epitopes located outside the receptor-binding region tend to have a negative NII. We cannot correlate the immune selfness of epitopes with NII because there is no good method to evaluate the immune selfness of conformational epitopes. Overall, in rational design of viral subunit vaccines, the epitopes with a high positive NII should be preserved and exposed, while those with a high negative NII should be eliminated via deletion or masking. Indeed, our study has identified an epitope containing Thr579 as one with a high negative NII on MERS-CoV RBD. Thr579 is located on a protruding loop and away from the receptor-binding region, both of which contribute to its high negative NII. Importantly, Thr579 is buried inside the full-length coronavirus spike proteins, and only becomes exposed on the surface of the recombinant MERS-CoV RBD vaccine as an outcome of subunit vaccine design. To overcome this limitation of subunit vaccine design, the newly exposed epitopes with a high negative NII need to be masked or deleted.

**[0119]** To apply the NII strategy to vaccine design, we successfully enhanced the efficacy of the MERS-CoV RBD vaccine in virus challenge studies by masking its strong negative epitope (i.e., the epitope containing Thr579, with an NII of -3.0) with a glycan probe. This engineered vaccine effectively protected hDPP4-transgenic mice from a lethal MERS-CoV infection. Compared with the wild type RBD vaccine, mice immunized with the engineered RBD vaccine showed increased neutralizing antibody responses in their sera; when challenged by MERS-CoV, they also demonstrated higher survival rate and less weight loss. These results prove that negative epitopes should be eliminated in vaccine design. In contrast, another engineered vaccine with a positive epitope masked (i.e., the epitope containing Arg511, with an NII of 0.6) showed reduced efficacy in virus challenge studies, confirming that positive epitopes should be preserved and exposed in vaccine design. Taken together, we validated both the significance and feasibility of the NII strategy in vaccine design by successfully engineering a variant form of the MERS-CoV RBD vaccine with significantly enhanced efficacy.

**[0120]** Overall, our study contributes to viral subunit vaccine design in the following ways. First, our study introduces a new concept neutralizing immunogenicity index for the evaluation of how individual epitopes contribute to the overall neutralizing immunogenicity of subunit vaccines. Previous studies could not evaluate the neutralizing immunogenicity of conformational B-cell epitopes that dominate coronavirus RBD vaccines. Second, using the NII strategy our study identified an immunodominant non-neutralizing epitope on the surface of the MERS-CoV RBD core structure. This result shows that exposure of previously buried epitopes on viral subunit vaccines poses a challenge for subunit vaccine design. This concept may be critical for the development of many viral RBD-based vaccines. Third, our study demonstrates that masking an immunodominant

non-neutralizing epitope with a negative NII value on the surface of the MERS-CoV RBD core structure can shift host immune responses towards the neutralizing epitopes in the RBM region, providing means to overcome the limitation of viral subunit vaccines from vaccine design. Previous studies showed that hypervariable regions on HIV gp120 divert host immune responses and that masking these regions can shift host immune responses towards conserved neutralizing epitopes, providing means to overcome the limitation of viral subunit vaccines from viral evolution. Fourth, although the NII strategy was used in the current study to improve the efficacy of viral subunit vaccines, it can also be potentially helpful in other epitope-based vaccine research. For example, previous studies masked or resurfaced non-neutralizing epitopes on viral immunogens, and used the engineered immunogens as baits to screen from neutralizing sera for monoclonal antibodies that bind to conserved neutralizing epitopes. It is conceivable that the NII strategy can help identify immunodominant non-neutralizing epitopes on immunogens, allowing more targeted epitope modifications for efficient antibody screening. Finally, our study suggests that a three-dimensional “neutralizing immunogenicity map” (NIM) can be drawn to describe the distribution of epitopes with different neutralizing immunogenicity on the surface of viral subunit vaccines. Such an NIM can guide targeted masking of multiple strong negative epitopes, further enhancing the efficacy of viral subunit vaccines.

**[0121]** Unless otherwise indicated, all numbers expressing quantities of ingredients, properties such as molecular weight, reaction conditions, and so forth used in the specification and claims are to be understood as being modified in all instances by the term “about.” Accordingly, unless indicated to the contrary, the numerical parameters set forth in the specification and attached claims are approximations that may vary depending upon the desired properties sought to be obtained by the present invention. At the very least, and not as an attempt to limit the application of the doctrine of equivalents to the scope of the claims, each numerical parameter should at least be construed in light of the number of reported significant digits and by applying ordinary rounding techniques. Notwithstanding that the numerical ranges and parameters setting forth the broad scope of the invention are approximations, the numerical values set forth in the specific examples are reported as precisely as possible. Any numerical value, however, inherently contains certain errors necessarily resulting from the standard deviation found in their respective testing measurements.

**[0122]** The terms “a,” “an,” “the” and similar referents used in the context of describing the invention (especially in the context of the following claims) are to be construed to cover both the singular and the plural, unless otherwise indicated herein or clearly contradicted by context. Recitation of ranges of values herein is merely intended to serve as a shorthand method of referring individually to each separate value falling within the range. Unless otherwise indicated herein, each individual value is incorporated into the specification as if it were individually recited herein. All methods described herein can be performed in any suitable order unless otherwise indicated herein or otherwise clearly contradicted by context. The use of any and all examples, or exemplary language (e.g., “such as”) provided herein is intended merely to better illuminate the invention and



does not pose a limitation on the scope of the invention otherwise claimed. No language in the specification should be construed as indicating any non-claimed element essential to the practice of the invention.

**[0123]** Groupings of alternative elements or embodiments of the invention disclosed herein are not to be construed as limitations. Each group member may be referred to and claimed individually or in any combination with other members of the group or other elements found herein. It is anticipated that one or more members of a group may be included in, or deleted from, a group for reasons of convenience and/or patentability. When any such inclusion or deletion occurs, the specification is deemed to contain the group as modified thus fulfilling the written description of all Markush groups used in the appended claims.

**[0124]** Certain embodiments of this invention are described herein, including the best mode known to the inventors for carrying out the invention. Of course, variations on these described embodiments will become apparent to those of ordinary skill in the art upon reading the foregoing description. The inventor expects skilled artisans to employ such variations as appropriate, and the inventors intend for the invention to be practiced otherwise than specifically described herein. Accordingly, this invention includes all modifications and equivalents of the subject matter recited in the claims appended hereto as permitted by applicable law. Moreover, any combination of the above-described elements in all possible variations thereof is encompassed by the invention unless otherwise indicated herein or otherwise clearly contradicted by context.

**[0125]** Specific embodiments disclosed herein may be further limited in the claims using consisting of or consisting essentially of language. When used in the claims, whether as filed or added per amendment, the transition term "consisting of" excludes any element, step, or ingredient not specified in the claims. The transition term "consisting essentially of" limits the scope of a claim to the specified materials or steps and those that do not materially affect the basic and novel characteristic(s). Embodiments of the invention so claimed are inherently or expressly described and enabled herein.

**[0126]** Furthermore, numerous references have been made to patents and printed publications throughout this specification. Each of the above-cited references and printed publications are individually incorporated herein by reference in their entirety.

**[0127]** In closing, it is to be understood that the embodiments of the invention disclosed herein are illustrative of the principles of the present invention. Other modifications that may be employed are within the scope of the invention. Thus, by way of example, but not of limitation, alternative configurations of the present invention may be utilized in accordance with the teachings herein. Accordingly, the present invention is not limited to that precisely as shown and described.

We claim:

1. A protein comprising:
  - a Middle East respiratory syndrome coronavirus (MERS-CoV) spike (S) protein sequence comprising amino acids 377-588 of the MERS-Co-V S protein with a T579N mutation; and
  - an immunopotentiator.
2. The protein of claim 1, wherein the immunopotentiator sequence is an Fc fragment of human IgG (Fc), a C3d protein, an *Onchocerca volvulus* ASP-1, a cholera toxin, a muramyl peptide, or a cytokine.
3. The protein of any one of claims 1 or 2, wherein the immunopotentiator is Fc.
4. The protein of claims 1 or 2, wherein the protein further comprises a stabilization sequence disposed between the MERS-CoV S protein sequence and the immunopotentiator sequence.
5. The protein of claim 4, wherein the stabilization sequence is a foldon (Fd) or GCN4.
6. The protein of claims 1 or 2, wherein the protein further comprises a linker sequence disposed between the MERS-CoV S protein sequence and the immunopotentiator sequence, and the linker is (GGGGS)<sub>n</sub>, wherein n is an integer between 0 and 8.
7. The protein according to claim 6, wherein n is 1.
8. The protein of any one of claims 1-7, wherein the protein is produced in a mammalian expression system.
9. The protein of claim 1, wherein the protein comprises the sequence of S377-588-Fc T579N (SEQ ID NO:26).
10. An immunogenic composition comprising a protein, the protein comprising:
  - an MERS-CoV S protein sequence comprising amino acids 377-588 of the MERS-Co-V S protein with a T579N mutation; and
  - an immunopotentiator.
11. The immunogenic composition of claim 10, wherein the immunopotentiator sequence is an Fc fragment of human IgG (Fc), a C3d, an *Onchocerca volvulus* ASP-1, a cholera toxin, a muramyl peptide, or a cytokine.
12. The immunogenic composition of claims 10 or 11, wherein the immunopotentiator is Fc.
13. The immunogenic composition of any one of claims 10 or 11, wherein the protein further comprises a stabilization sequence disposed between the MERS-CoV S protein sequence and the immunopotentiator sequence.

14. The immunogenic composition of claim 13, wherein the stabilization sequence is a foldon (Fd) or GCN4.

15. The immunogenic composition of claims 10 or 11, wherein the protein further comprises a linker sequence disposed between the MERS-CoV S protein sequence and the immunopotentiator sequence, and the linker is (GGGGS)<sub>n</sub>, wherein n is an integer between 0 and 8.

16. The immunogenic composition of claim 15, wherein n is 1.

17. The immunogenic composition of any one of claims 10-16, wherein the protein is produced in a mammalian expression system.

18. The immunogenic composition of claim 10, wherein the protein comprises the sequence of S377-588-Fc T579N (SEQ ID NO:26).

19. The immunogenic composition of any one of claims 1-18 further comprising at least one pharmaceutically acceptable excipient.

20. The immunogenic composition of any one of claims 10-19, further comprising an adjuvant.

21. A method of inducing a protective immune response against MERS-CoV comprising:  
administering the immunogenic composition of claim 10 or the protein of claim 1 to a subject in need thereof;

wherein the immunogenic composition induces a protective immune response against challenge with MERS-CoV in the host.

22. The method according to claim 21, wherein the immunogenic composition further comprises an adjuvant.

23. The method according to claims 21 or 22, wherein the administering step comprises a prime immunization and at least one boost immunization.

24. The method according to claim 23, wherein the boost immunizations are administered at least twice.

25. The method according to claim 24, wherein the boost immunizations are administered weekly, every other week, monthly, or every other month.

26. The method according to claim 24, wherein the boost immunizations are administered weekly, every 2 weeks, every 3 weeks, every 4 weeks, every 5 weeks, every 6 weeks, every 7 weeks, every 8 weeks, every 9 weeks, every 10 weeks, every 11 weeks, or every 12 weeks.

27. Use of the immunogenic composition according to any one of claims 10-20 to induce a protective immune response against a MERS-CoV.

28. The use according to claim 27, wherein the immunogenic composition further comprises an adjuvant.

29. The use according to claims 27 or 28, wherein the administering step comprises a prime immunization and at least one boost immunization.

30. The use according to claim 29, wherein the boost immunizations are administered at least twice.

31. The use according to claim 30, wherein the boost immunizations are administered weekly, every other week, monthly, or every other month.

32. The method according to claim 30, wherein the boost immunizations are administered weekly, every 2 weeks, every 3 weeks, every 4 weeks, every 5 weeks, every 6 weeks, every 7 weeks, every 8 weeks, every 9 weeks, every 10 weeks, every 11 weeks, or every 12 weeks.

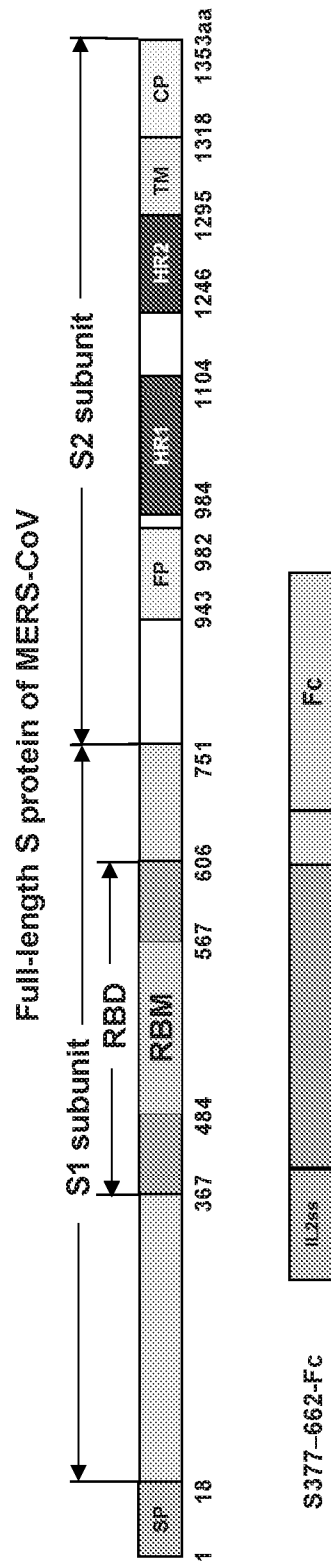


FIG. 1

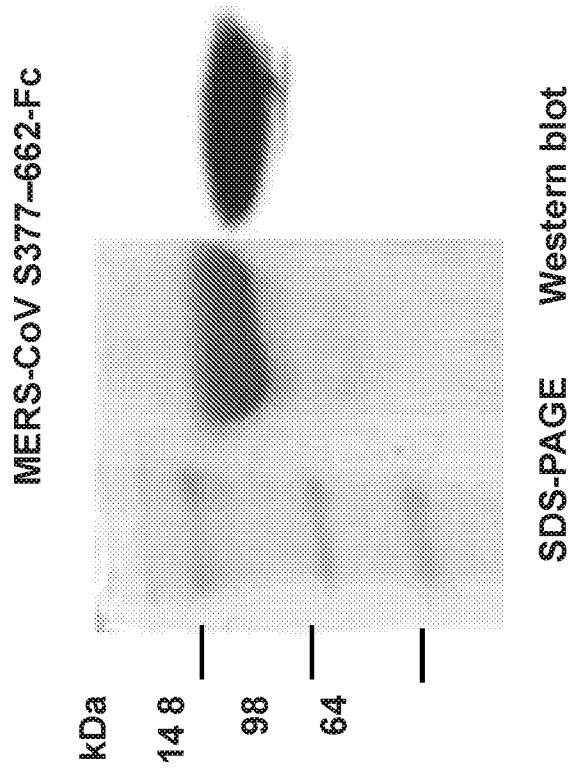


FIG. 2

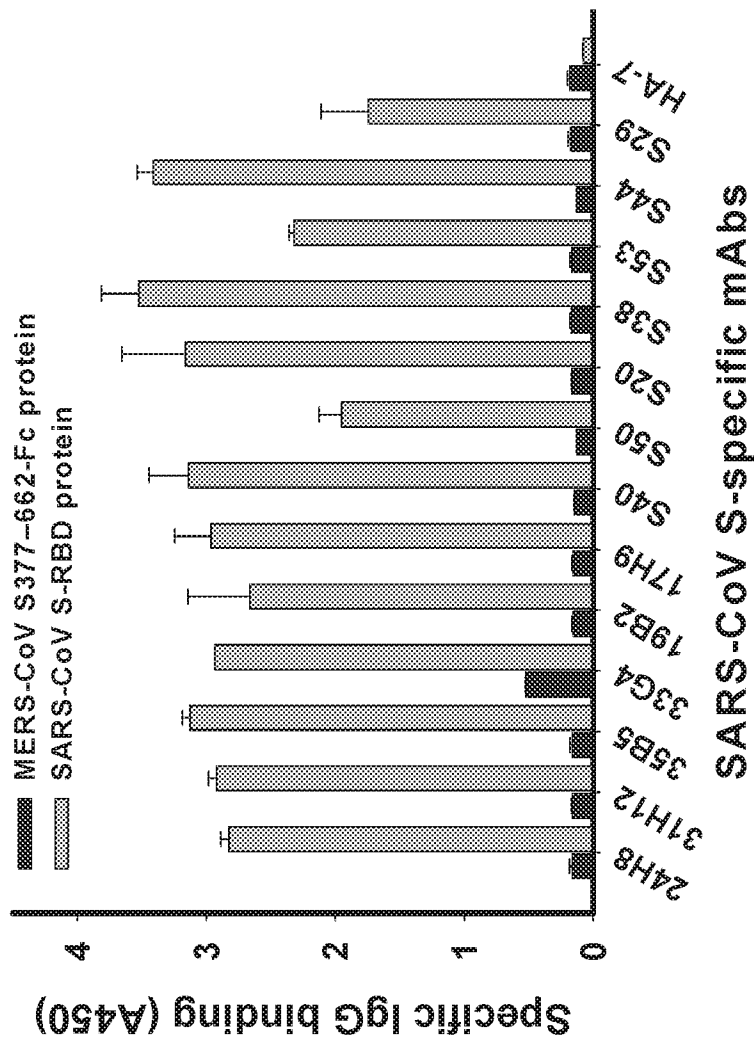


FIG. 3

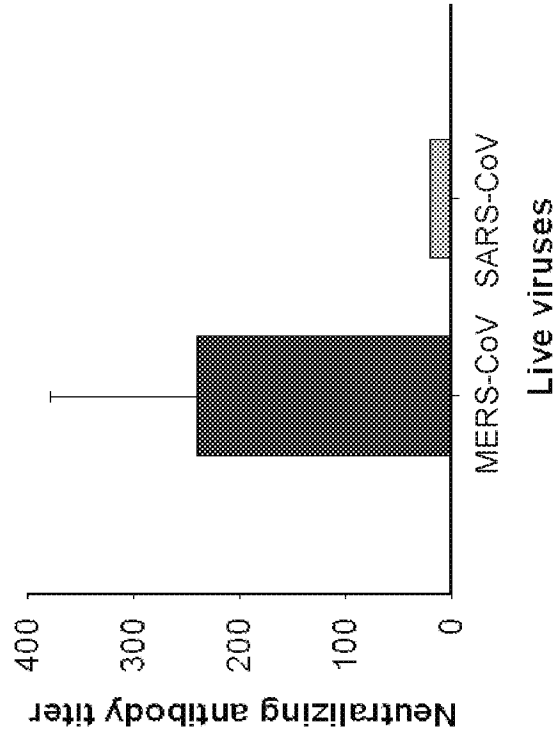


FIG. 4B

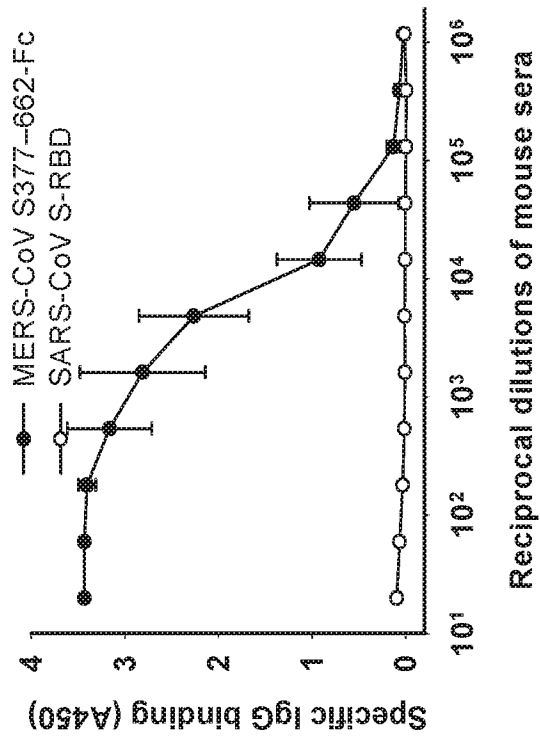


FIG. 4A



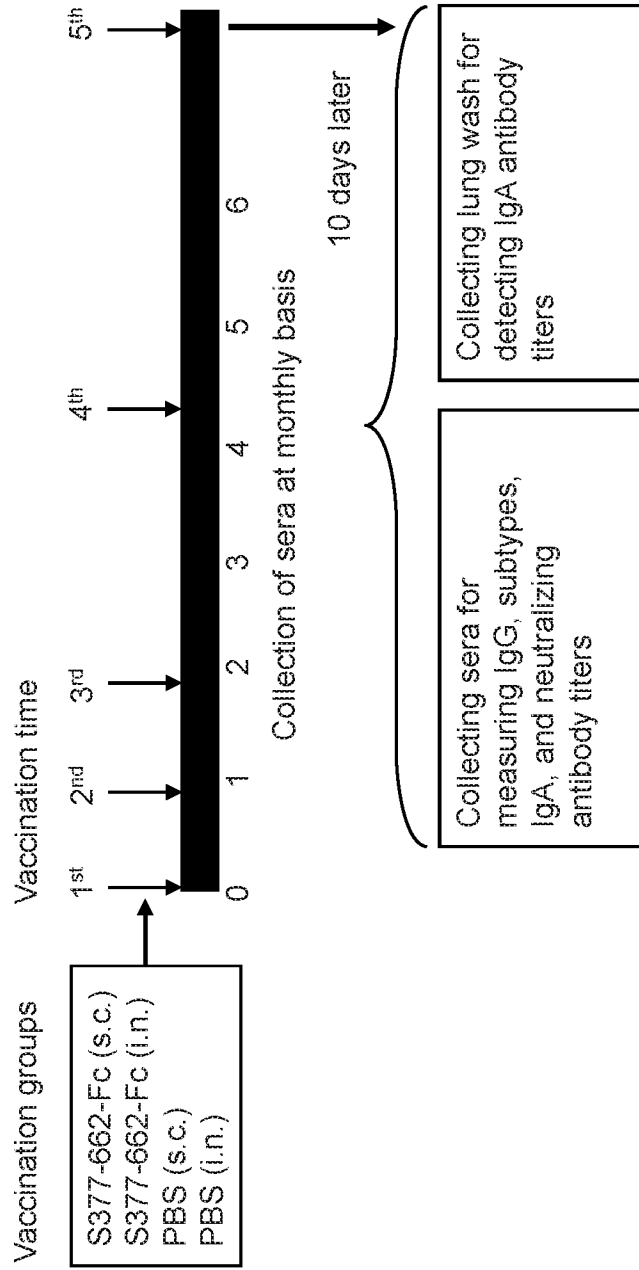


FIG. 5

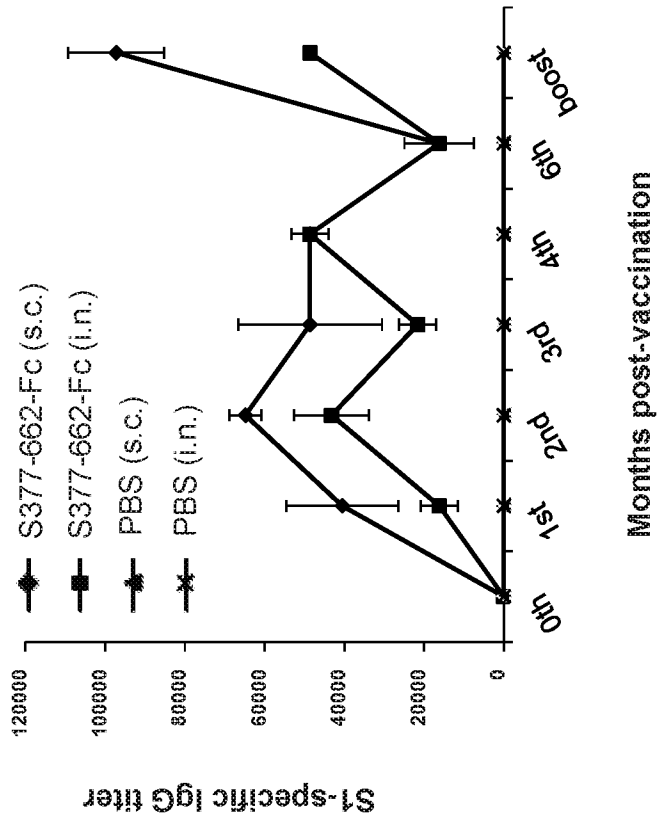


FIG. 6B

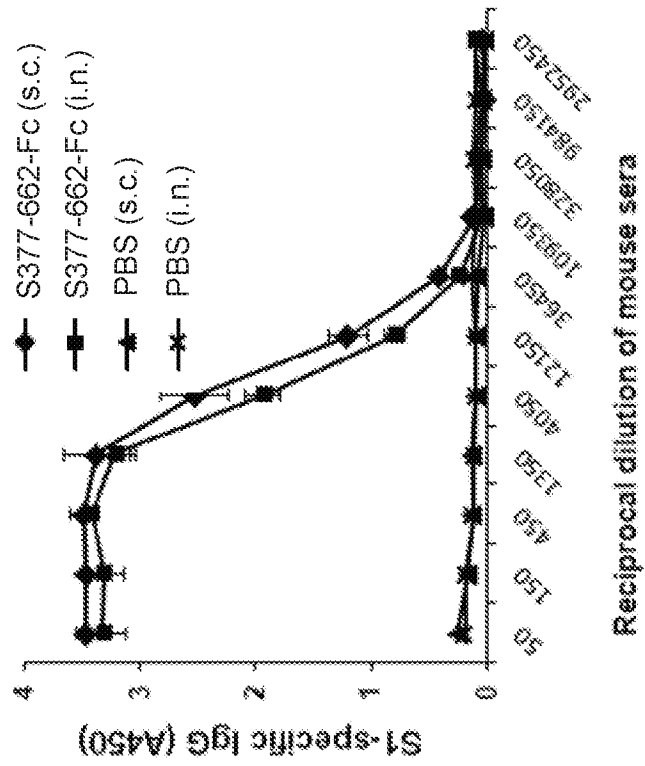


FIG. 6A

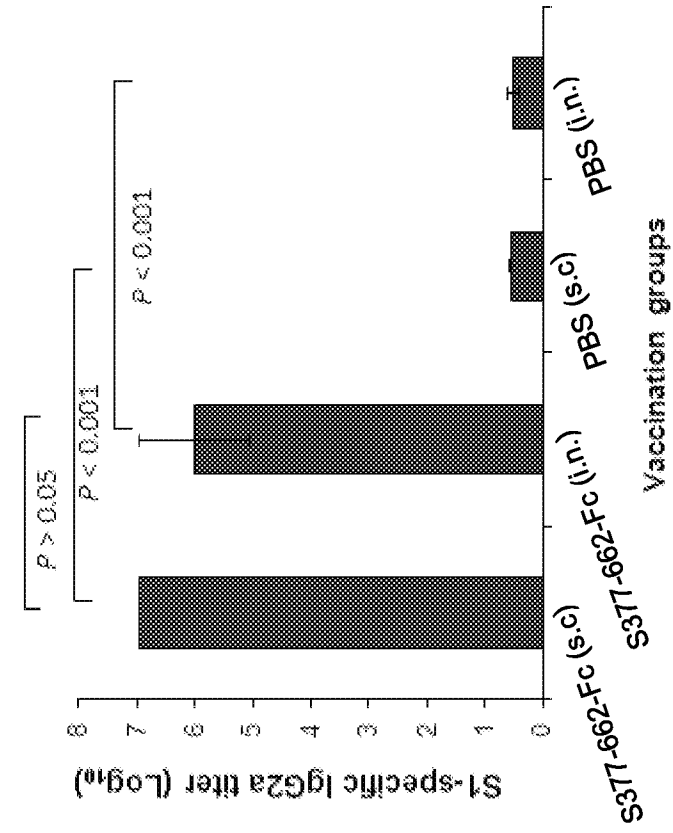


FIG. 7B

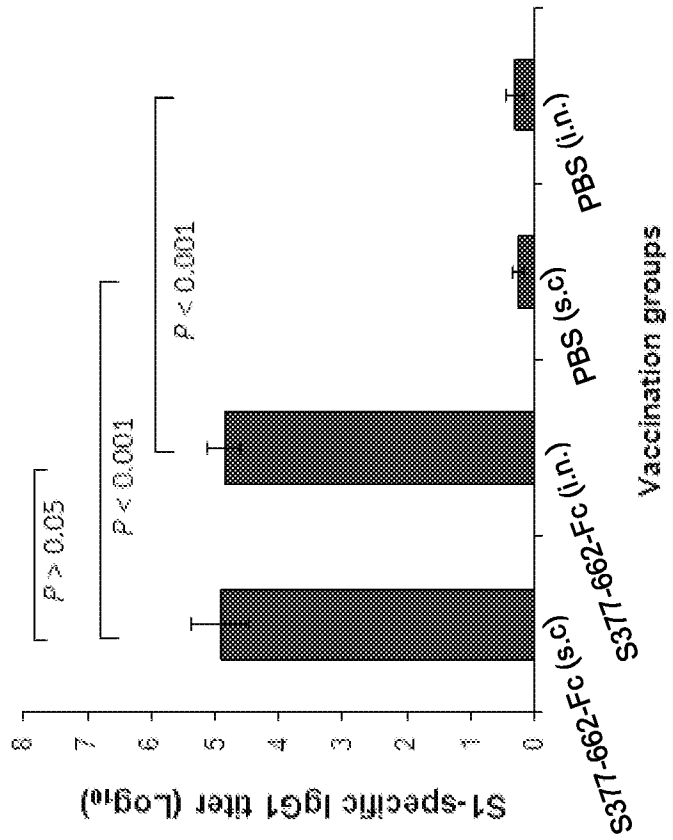


FIG. 7A

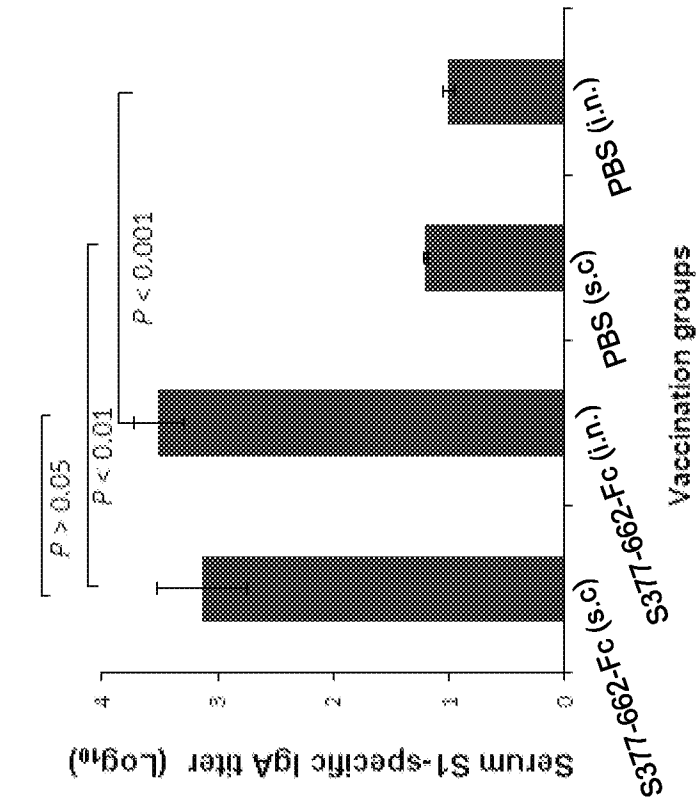


FIG. 8B

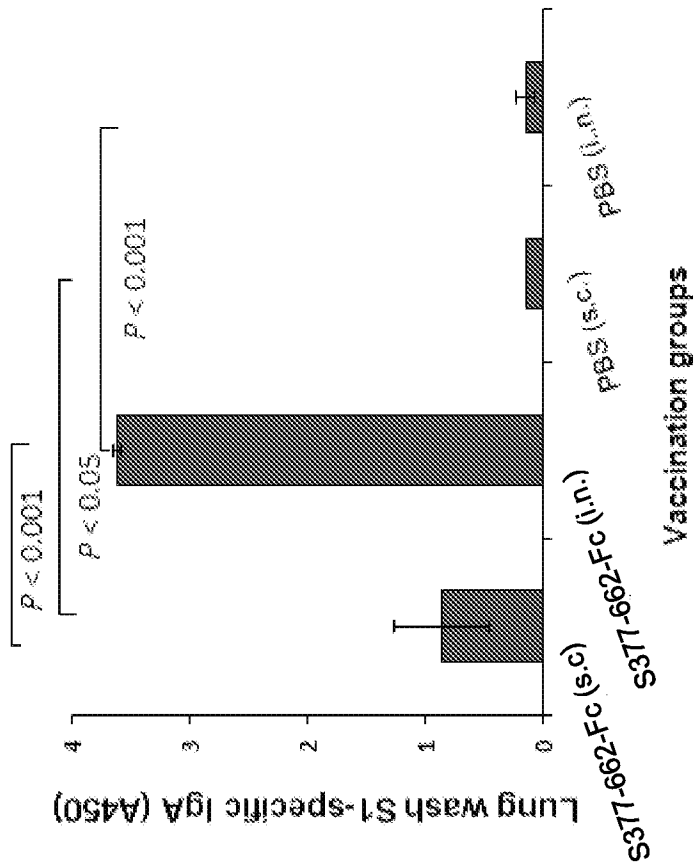


FIG. 8A

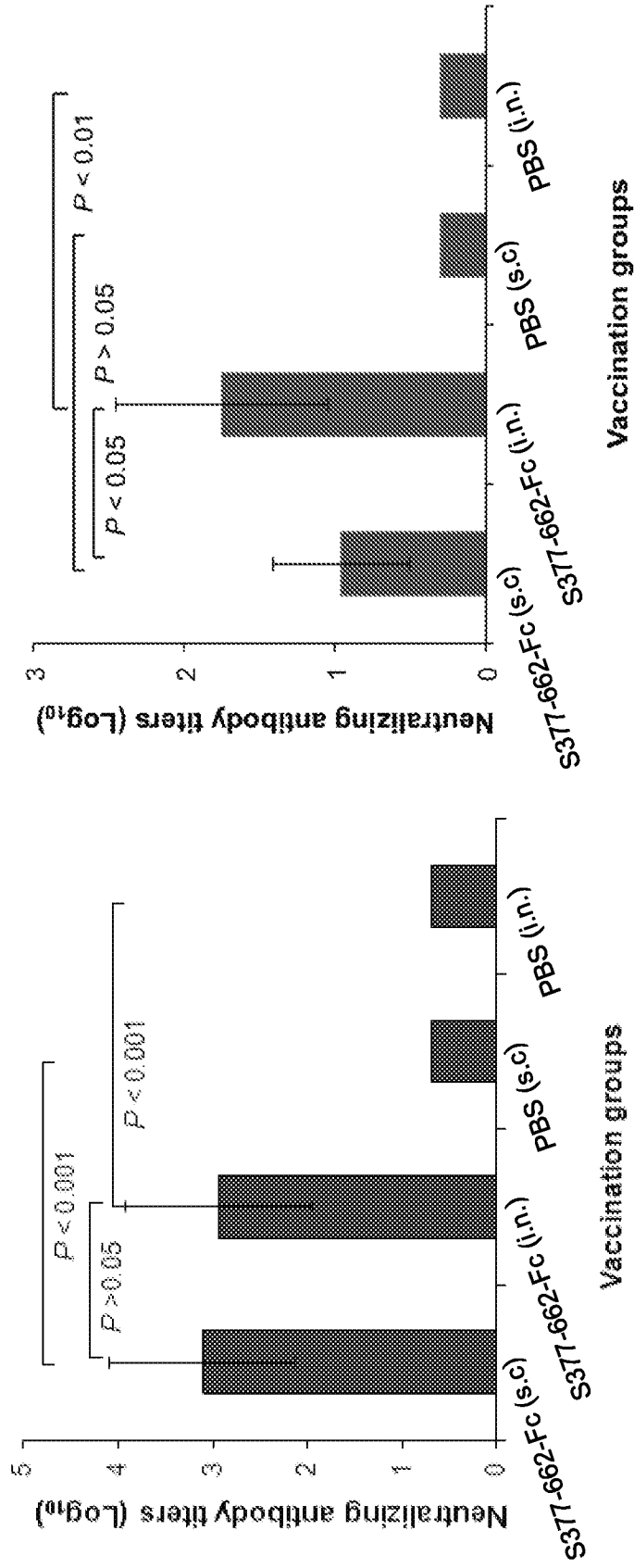


FIG. 9A

FIG. 9B

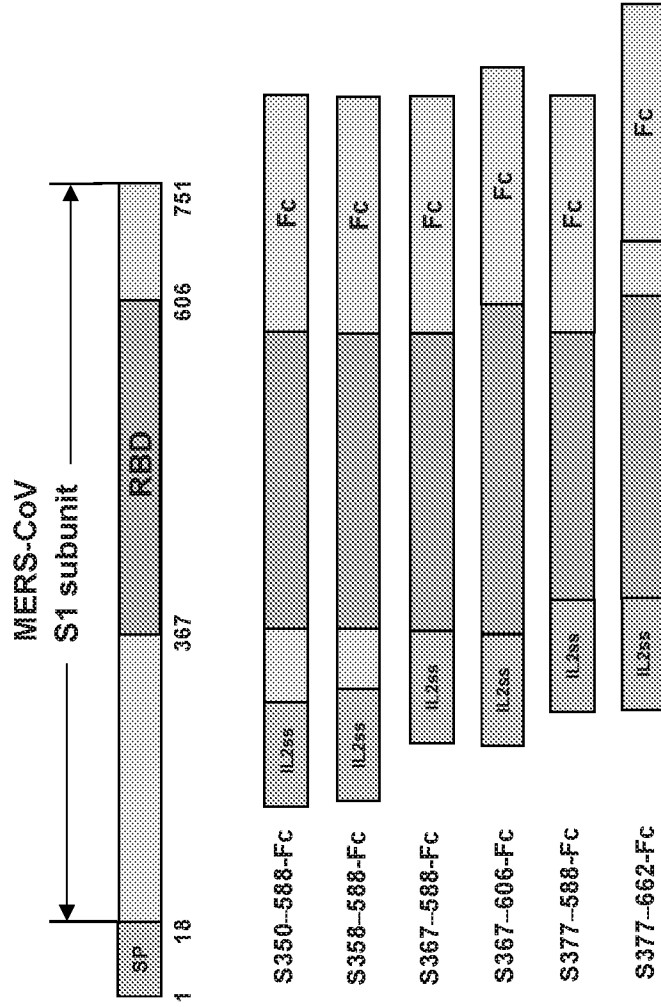
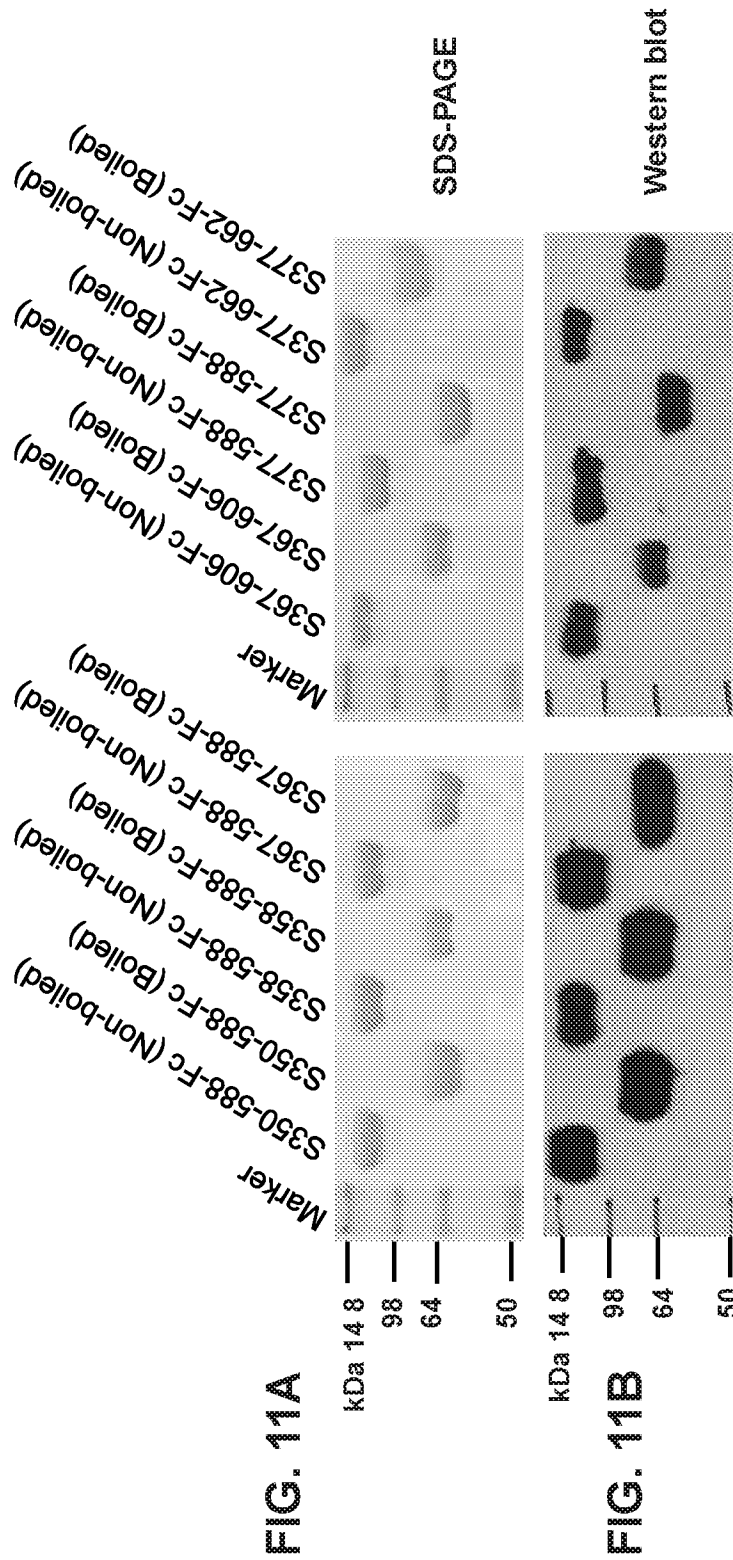


FIG. 10A

FIG. 10B

11/25



12/25

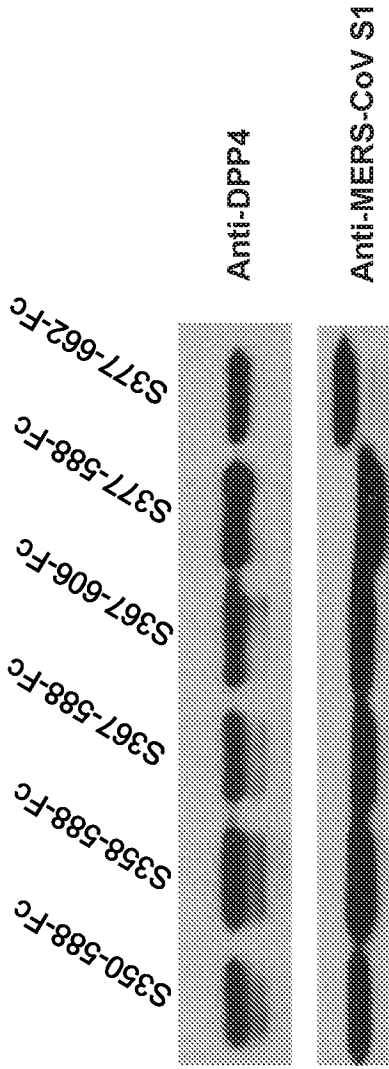


FIG. 12A

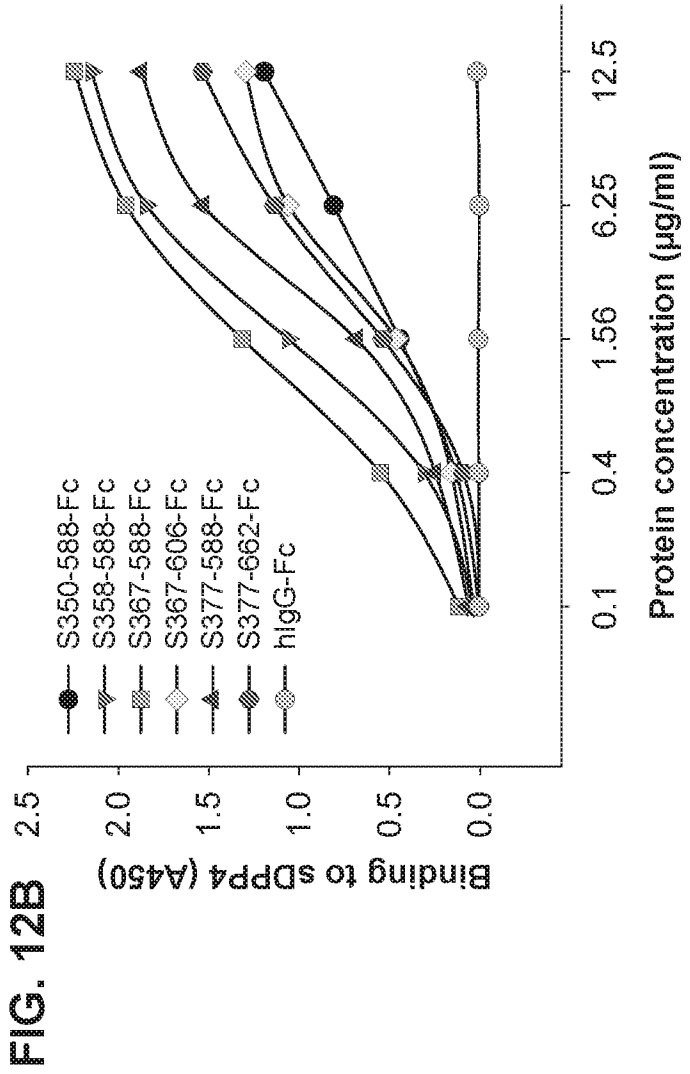


FIG. 12B



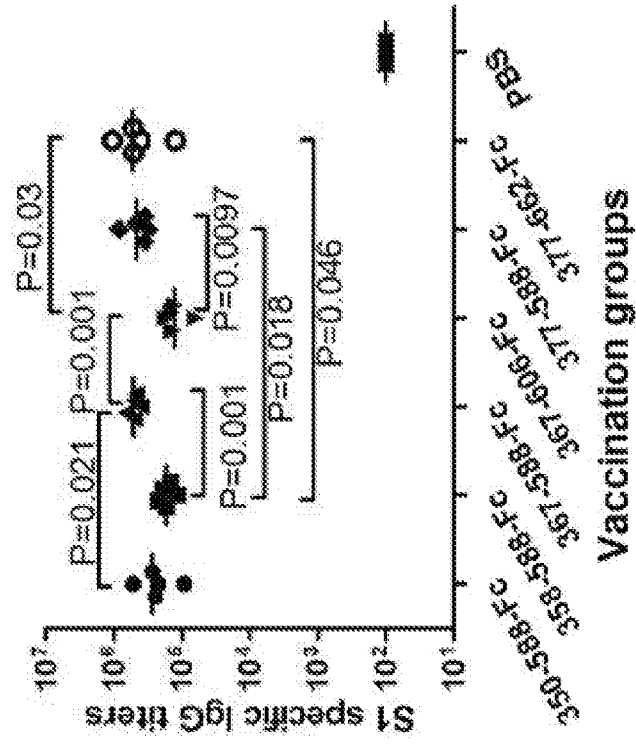


FIG. 13B

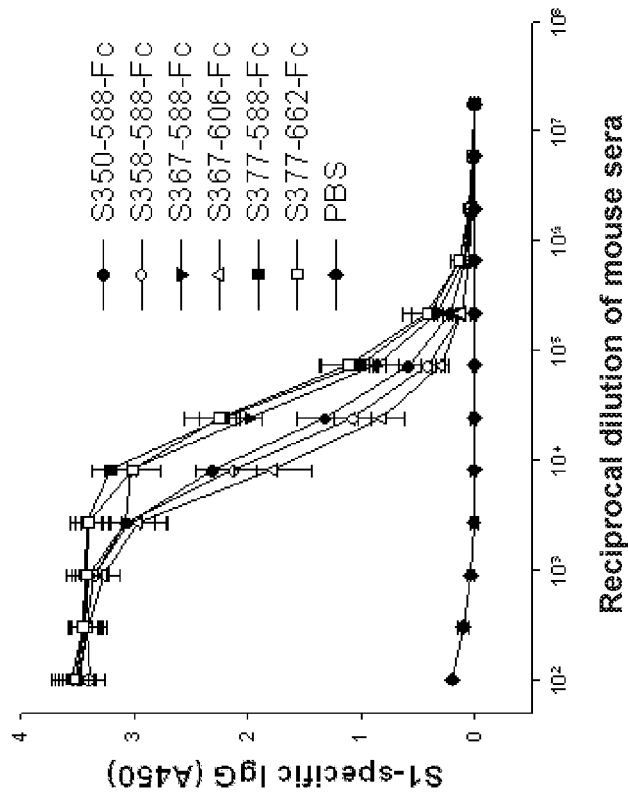


FIG. 13A

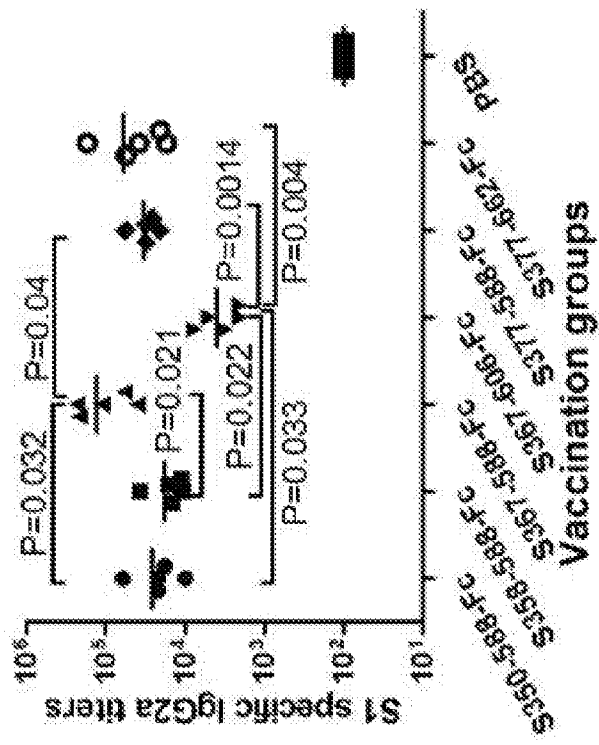


FIG. 14

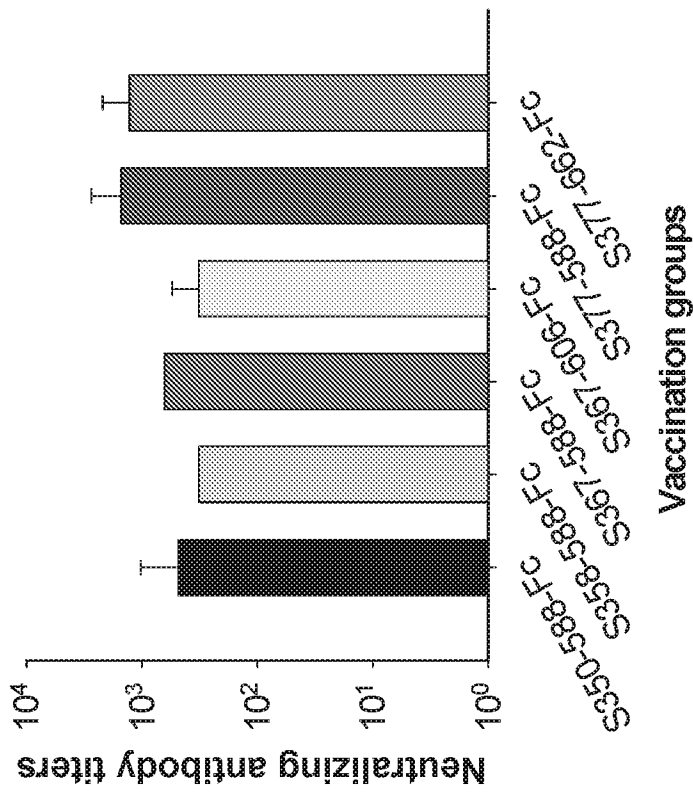


FIG. 15

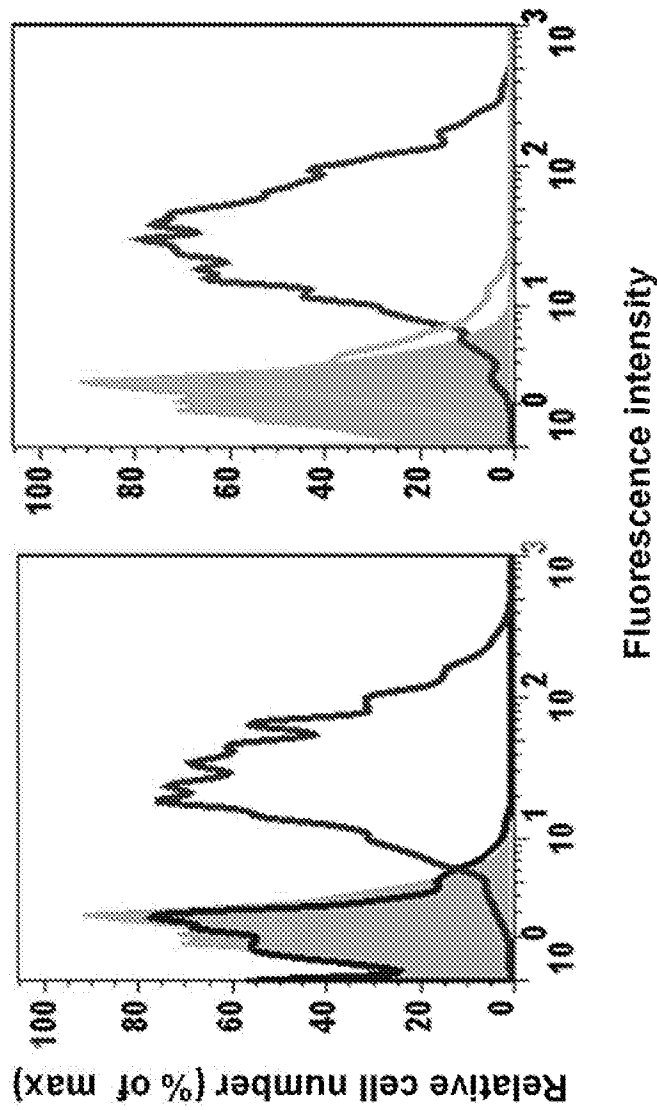


FIG. 16A

FIG. 16B

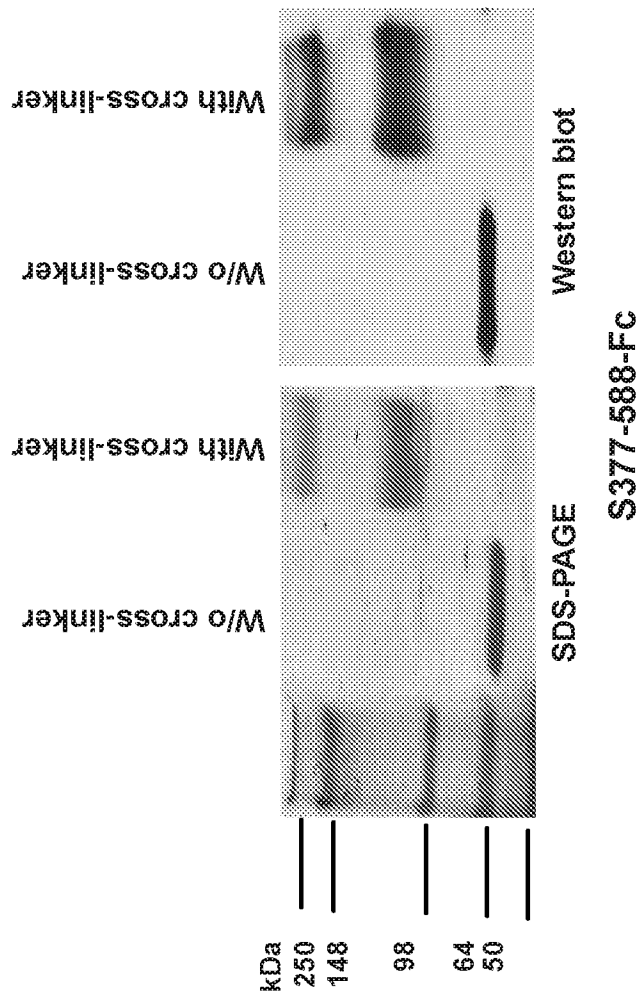


FIG. 17

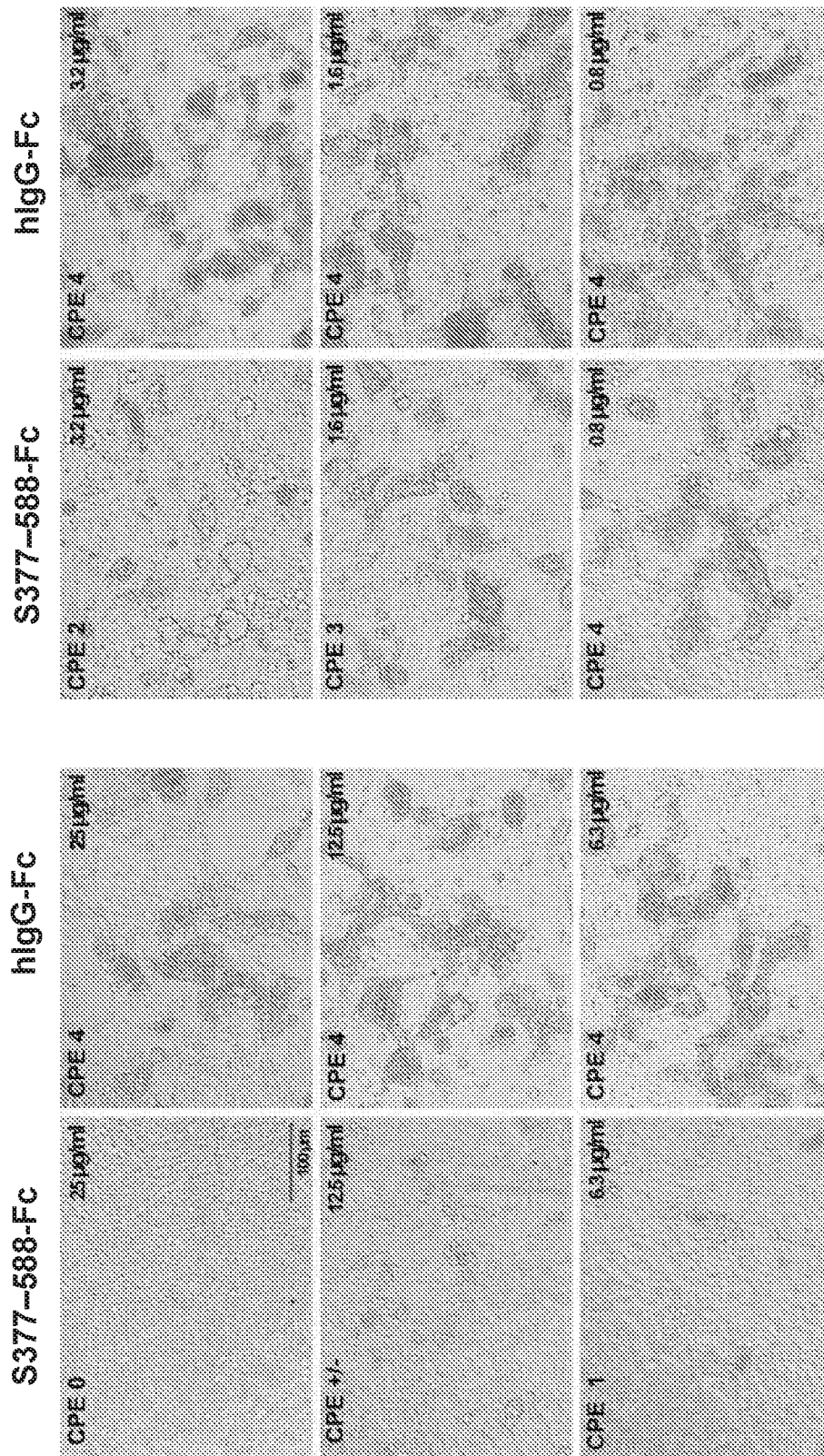


FIG. 18

FIG. 19B

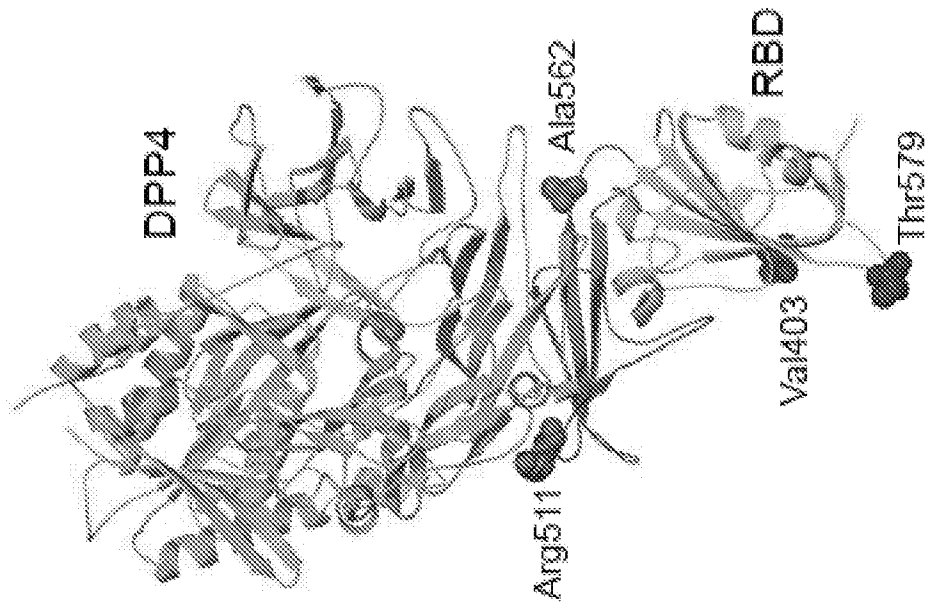


FIG. 19A

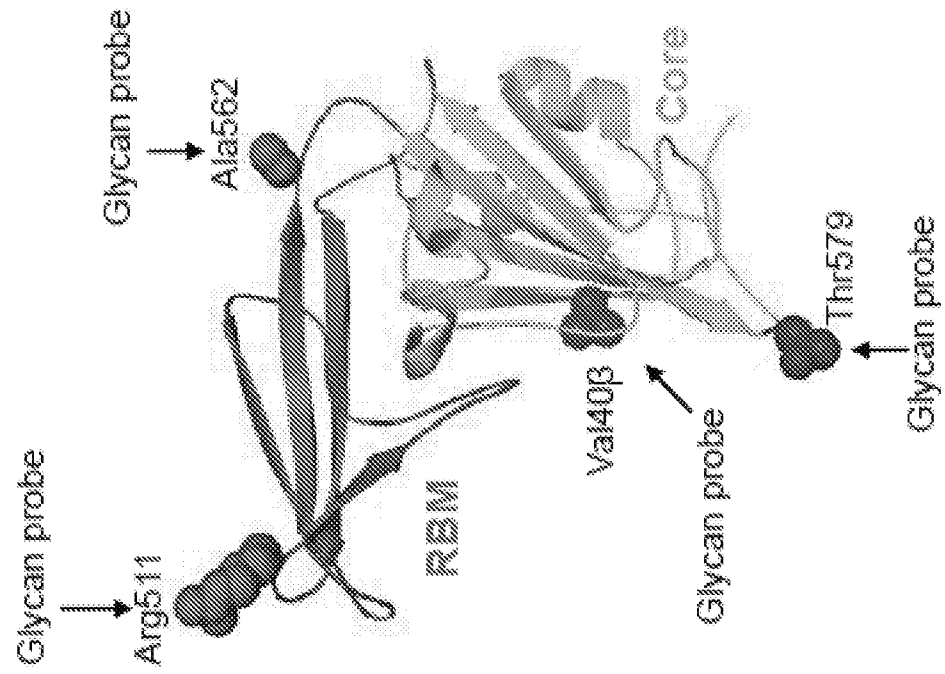


FIG. 19D

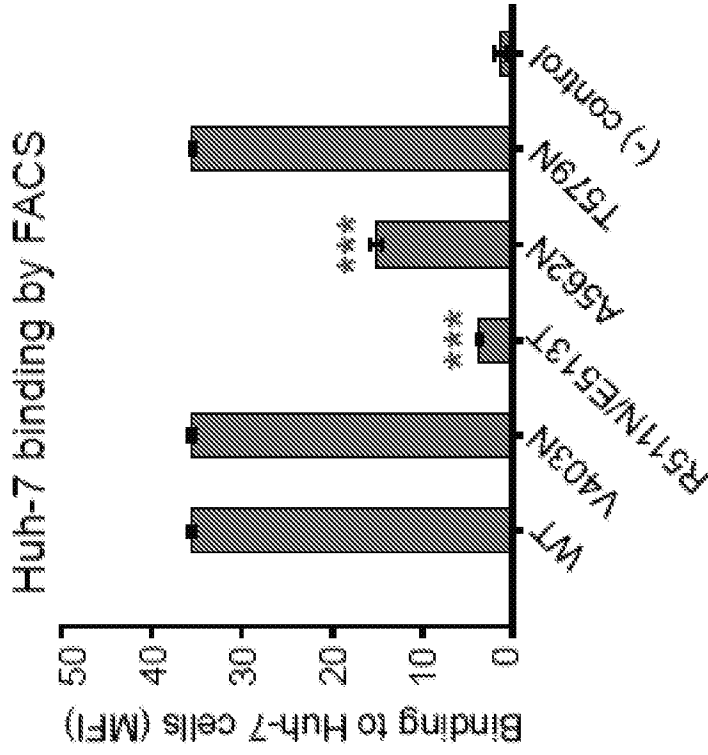


FIG. 19C

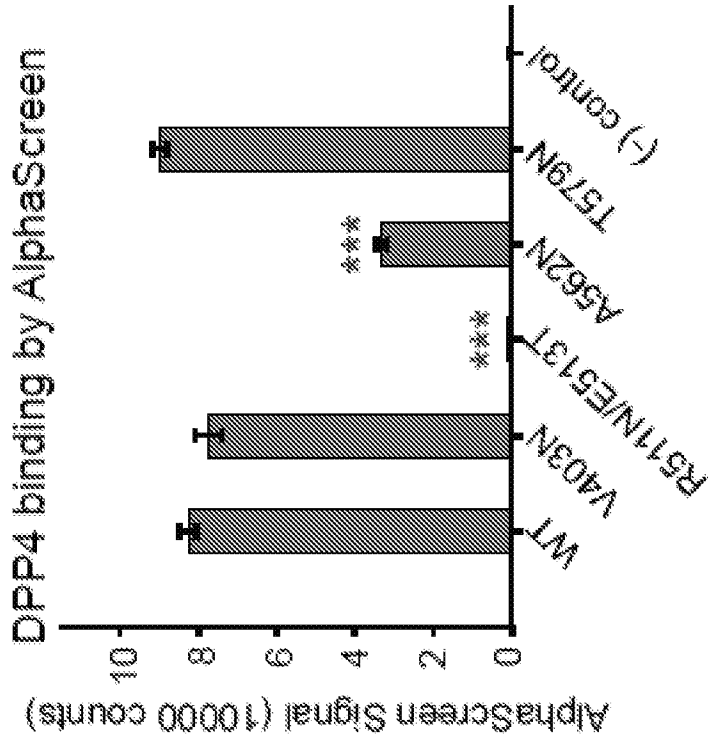




FIG. 20B

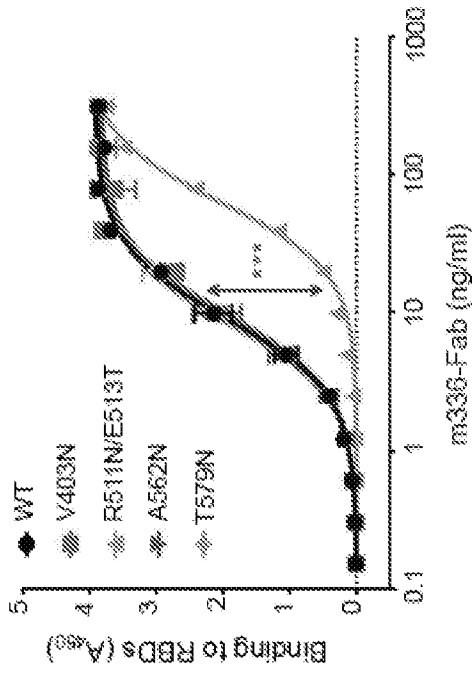


FIG. 20A

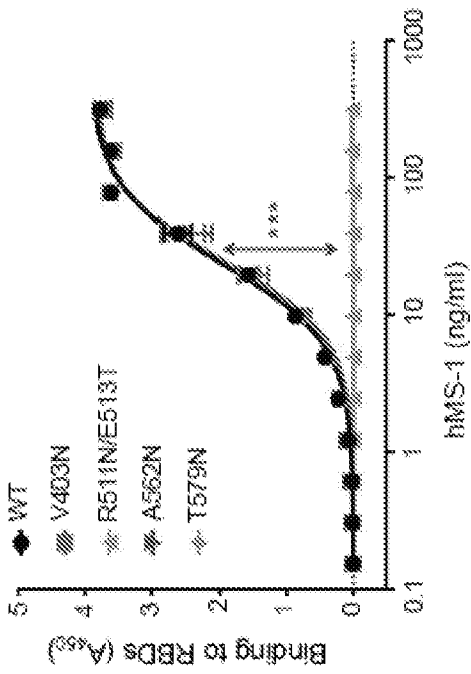


FIG. 20D

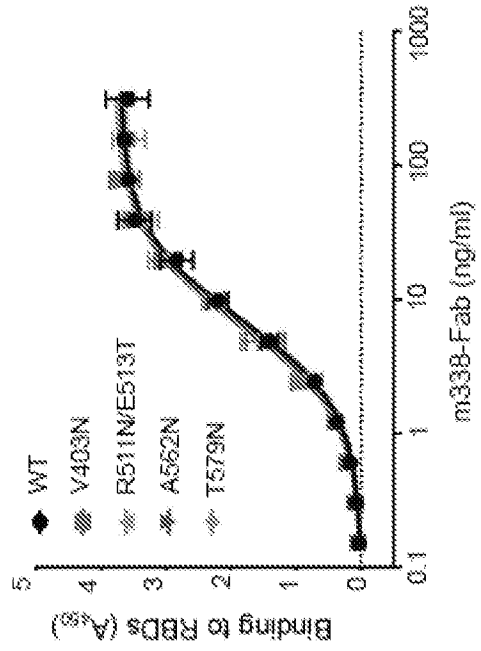
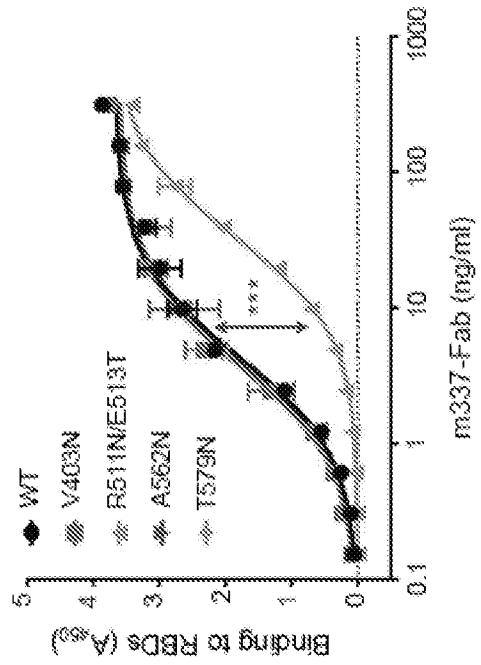


FIG. 20C



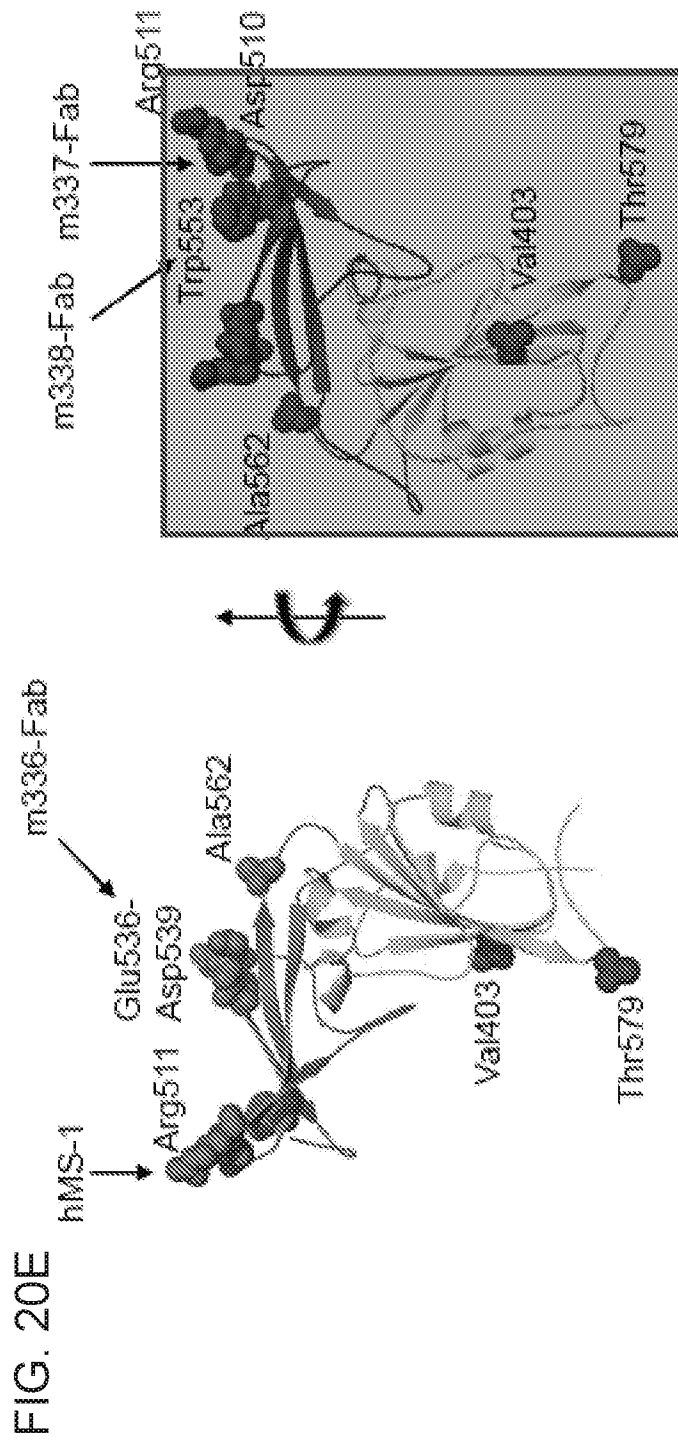


FIG. 21A

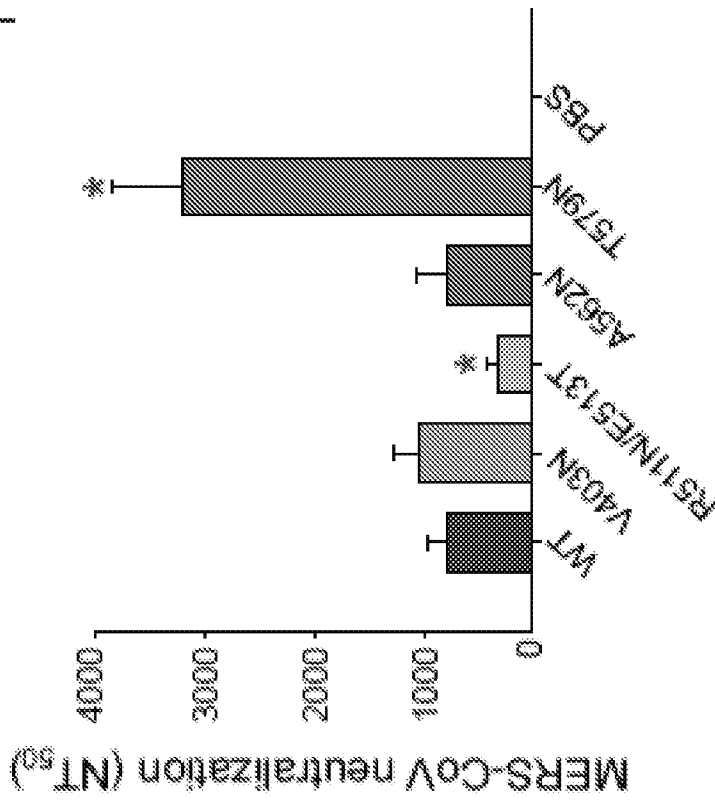


FIG. 21C

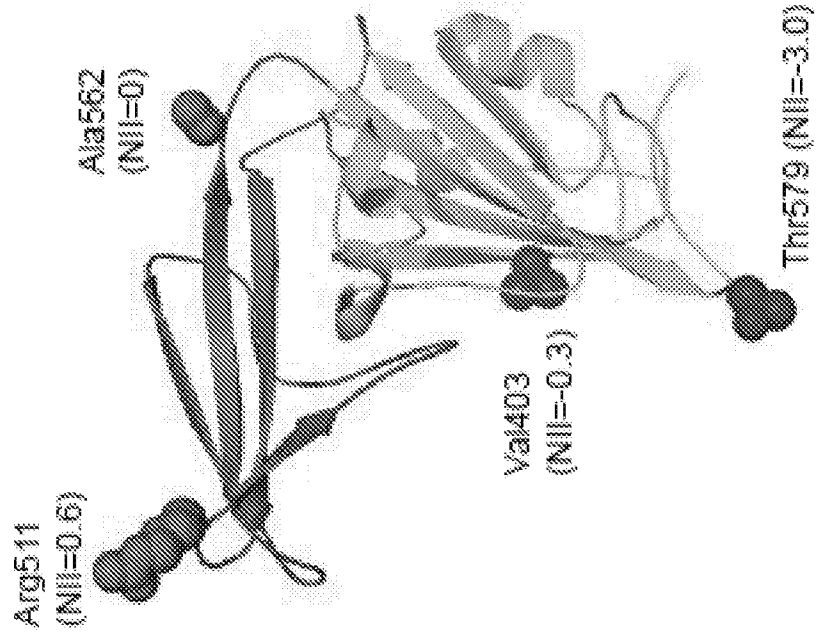


FIG. 21B

Neutralizing immunogenicity index (NII)

$$= (NT_{50-wt} - NT_{50-probe}) / NT_{50-wt}$$

FIG. 22A

hMS-1 mAb

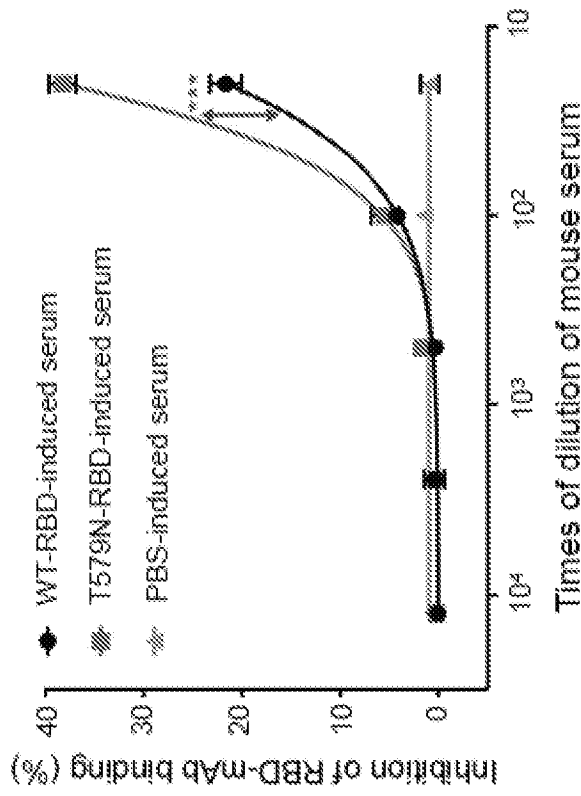


FIG. 22B

m336-Fab mAb

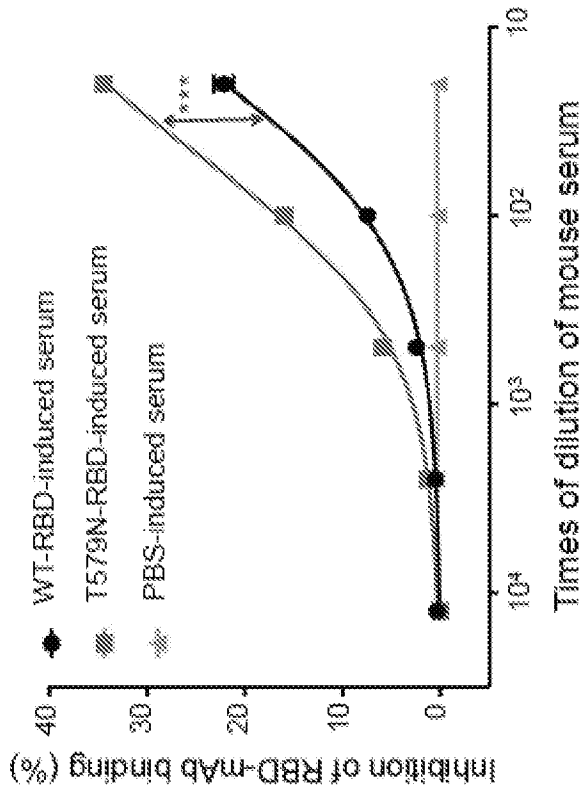


FIG. 23B

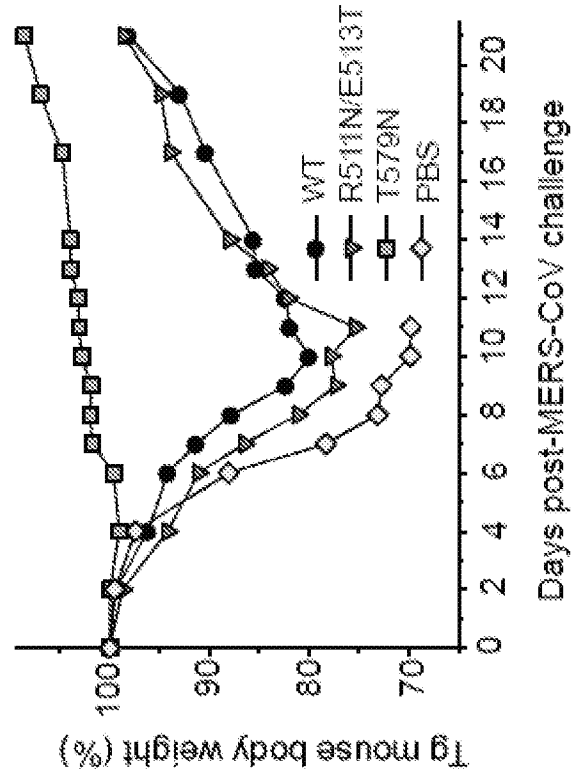
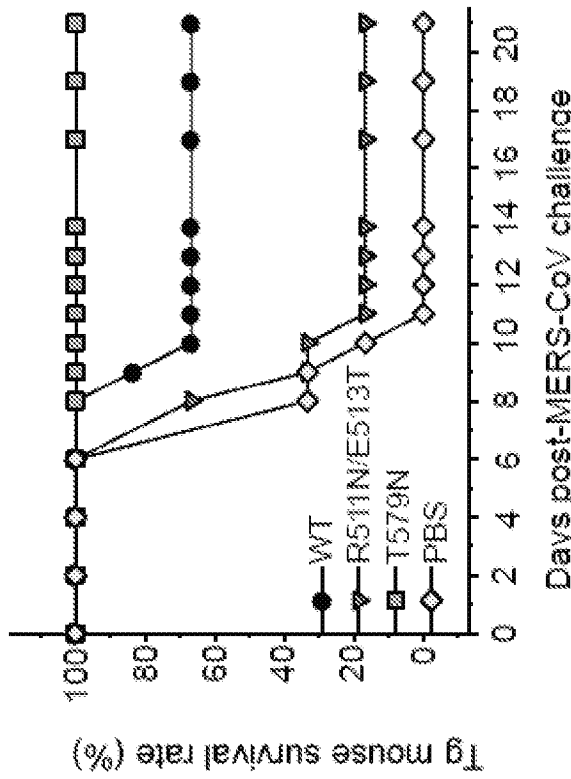


FIG. 23A



INTERNATIONAL SEARCH REPORT

International application No.

PCT/US2017/062354

A. CLASSIFICATION OF SUBJECT MATTER

IPC(8) - A61K 39/215; A61K 47/64; C07K 14/165; C12N 7/00 (2018.01)

CPC - A61K 47/646; C07K 14/165; C12N 2770/20021; C12N 2770/20022; C12N 2770/20034 (2018.01)

According to International Patent Classification (IPC) or to both national classification and IPC

B. FIELDS SEARCHED

Minimum documentation searched (classification system followed by classification symbols)

See Search History document

Documentation searched other than minimum documentation to the extent that such documents are included in the fields searched

USPC - 424/93.2; 424/193.1; 424/221.1; 514/1.5 (keyword delimited)

Electronic data base consulted during the international search (name of data base and, where practicable, search terms used)

See Search History document

C. DOCUMENTS CONSIDERED TO BE RELEVANT

Category*	Citation of document, with indication, where appropriate, of the relevant passages	Relevant to claim No.
A	US 2016/0296617 A1 (ZHOU et al) 13 October 2016 (13.10.2016) entire document	1-7, 9-16, 18, 21, 22
A	• KIM et al. "Variations in Spike Glycoprotein Gene of MERS-CoV, South Korea, 2015," Emerging Infectious Diseases, 31 January 2016 (31.01.2016), Vol. 22, No. 1, Pgs. 100-104. entire document	1-7, 9-16, 18, 21, 22
A	• KIM et al. "Spread of Mutant Middle East Respiratory Syndrome Coronavirus with Reduced Affinity to Human CD26 during the South Korean Outbreak," mBio, 01 March 2016 (01.03.2016), Vol. 7, No. 2:e00019-16, Pgs. 1-8. entire document	1-7, 9-16, 18, 21, 22
A	US 2016/0206729 A1 (NOVAVAX INC) 21 July 2016 (21.07.2016) entire document	1-7, 9-16, 18, 21, 22
A	WO 2016/138160 A1 (THE UNITED STATES OF AMERICA, AS REPRESENTED BY THE SECRETARY, DEPARTMENT OF HEALTH AND HUMAN SERVICES) 01 September 2016 (01.09.2016) entire document	1-7, 9-16, 18, 21, 22
A	WO 2015/143335 A1 (THE UNIVERSITY OF NORTH CAROLINA AT CHAPEL HILL) 24 September 2015 (24.09.2015) entire document	1-7, 9-16, 18, 21, 22
P, X	• DU et al. "Introduction of neutralizing immunogenicity index to the rational design of MERS coronavirus subunit vaccines," Nature Communications, 22 November 2016 (22.11.2016), Vol. 7:13473, Pgs. 1-9. entire document	1-7, 9-16, 18, 21, 22

Further documents are listed in the continuation of Box C.

See patent family annex.

\* Special categories of cited documents:

"A" document defining the general state of the art which is not considered to be of particular relevance

"E" earlier application or patent but published on or after the international filing date

"L" document which may throw doubts on priority claim(s) or which is cited to establish the publication date of another citation or other special reason (as specified)

"O" document referring to an oral disclosure, use, exhibition or other means

"P" document published prior to the international filing date but later than the priority date claimed

"T" later document published after the international filing date or priority date and not in conflict with the application but cited to understand the principle or theory underlying the invention

"X" document of particular relevance; the claimed invention cannot be considered novel or cannot be considered to involve an inventive step when the document is taken alone

"Y" document of particular relevance; the claimed invention cannot be considered to involve an inventive step when the document is combined with one or more other such documents, such combination being obvious to a person skilled in the art

"&" document member of the same patent family

Date of the actual completion of the international search

24 January 2018

Date of mailing of the international search report

23 FEB 2018

Name and mailing address of the ISA/US

Mail Stop PCT, Attn: ISA/US, Commissioner for Patents  
P.O. Box 1450, Alexandria, VA 22313-1450  
Facsimile No. 571-273-8300

Authorized officer

Blaine R. Copenheaver

PCT Helpdesk: 571-272-4300  
PCT OSP: 571-272-7774

INTERNATIONAL SEARCH REPORT

International application No.

PCT/US2017/062354

Box No. I Nucleotide and/or amino acid sequence(s) (Continuation of item 1.c of the first sheet)

1. With regard to any nucleotide and/or amino acid sequence disclosed in the international application, the international search was carried out on the basis of a sequence listing:
- a.  forming part of the international application as filed:
    - in the form of an Annex C/ST.25 text file.
    - on paper or in the form of an image file.
  - b.  furnished together with the international application under PCT Rule 13ter.1(a) for the purposes of international search only in the form of an Annex C/ST.25 text file.
  - c.  furnished subsequent to the international filing date for the purposes of international search only:
    - in the form of an Annex C/ST.25 text file (Rule 13ter.1(a)).
    - on paper or in the form of an image file (Rule 13ter.1(b) and Administrative Instructions, Section 713).
2.  In addition, in the case that more than one version or copy of a sequence listing has been filed or furnished, the required statements that the information in the subsequent or additional copies is identical to that forming part of the application as filed or does not go beyond the application as filed, as appropriate, were furnished.

3. Additional comments:

SEQ ID NO: 26 was searched.

INTERNATIONAL SEARCH REPORT

International application No.

PCT/US2017/062354

**Box No. II Observations where certain claims were found unsearchable (Continuation of item 2 of first sheet)**

This international search report has not been established in respect of certain claims under Article 17(2)(a) for the following reasons:

- 1.  Claims Nos.:  
because they relate to subject matter not required to be searched by this Authority, namely:
  
- 2.  Claims Nos.:  
because they relate to parts of the international application that do not comply with the prescribed requirements to such an extent that no meaningful international search can be carried out, specifically:
  
- 3.  Claims Nos.: 8, 17, 19, 20, 23-32  
because they are dependent claims and are not drafted in accordance with the second and third sentences of Rule 6.4(a).

**Box No. III Observations where unity of invention is lacking (Continuation of item 3 of first sheet)**

This International Searching Authority found multiple inventions in this international application, as follows:

- 1.  As all required additional search fees were timely paid by the applicant, this international search report covers all searchable claims.
- 2.  As all searchable claims could be searched without effort justifying additional fees, this Authority did not invite payment of additional fees.
- 3.  As only some of the required additional search fees were timely paid by the applicant, this international search report covers only those claims for which fees were paid, specifically claims Nos.:
  
- 4.  No required additional search fees were timely paid by the applicant. Consequently, this international search report is restricted to the invention first mentioned in the claims; it is covered by claims Nos.:

- Remark on Protest**
- The additional search fees were accompanied by the applicant's protest and, where applicable, the payment of a protest fee.
  - The additional search fees were accompanied by the applicant's protest but the applicable protest fee was not paid within the time limit specified in the invitation.
  - No protest accompanied the payment of additional search fees.